Carbon science perspective in 2022: Current research and future challenges

Vincent Meunier[1,2], Conchi Ania[3], Alberto Bianco[4], Yuan Chen[5], Go bong Choi[6], Yoon Ahm Kim[6], Nikhil Koratkar[2,7], Chang Liu[8], Juan M.D. Tascon[9], Mauricio Terrones[10]

1. Department of Physics, Applied Physics, and Astronomy. Rensselaer Polytechnic Institute, 110 8th Street, Troy, NY, 12180, USA
2. Department of Materials Science & Engineering. Rensselaer Polytechnic Institute, 110 8th Street, Troy, NY, 12180, USA
3. CEMHTI, CNRS (UPR 3079), Université d′Orléans, 45071 Orléans, France
4. CNRS, UPR3572, Immunology, Immunopathology and Therapeutic Chemistry, ISIS, University of Strasbourg, 67000 Strasbourg, France
5. The School of Chemical and Biochemical Engineering. the University of Sydney, NSW, 2006, Australia
6. Alan G. MacDiarmid Energy Research Institute, Chonnam National University, 77 Yongbong-ro, Buk-gu, Gwangju, Korea
7. Department of Mechanical, Aerospace and Nuclear Engineering, Rensselaer Polytechnic Institute, 110 8th Street, Troy, NY, 12180, USA
8. Shenyang National Laboratory for Materials Science, Institute of Metal Research, Chinese Academy of Sciences, Shenyang 110016, China
9. Instituto de Ciencia y Tecnología del Carbono, INCAR-CSIC, F. Pintado Fe 26, 33011 Oviedo, Spain
10. Department of Physics, Department of Chemistry, Department of Materials Science and Engineering and Center for 2-Dimensional and Layered Materials, 104 Davey Lab. the Pennsylvania State University, University Park, PA, 16802, USA

Introduction

Since 2016, the editors of *Carbon* have published a biennial *Perspectives* article where selected topics are discussed regarding current developments in carbon material research [1–3]. Since 2020, a new Elsevier journal ("Carbon Trends") was launched by Editors of Carbon, to broaden the opportunities for scientists and engineers to share the fruit of their research on carbon materials and to offer a full open-access vehicle to do so. For this reason, this year, the Editors of *Carbon* are now joined by the Editor-in-Chief of *Carbon Trends* to address current and upcoming challenges in carbon material science. This document does not have the ambition to present an exhaustive review of the field. Instead, it is an attempt to highlight selected topics that the editors consider relevant with strong potential for growth and development in the field of materials science and engineering applied to carbon systems. The emphasis is placed on very recent developments, including – but not limited to – research published in both journals.

Carbon has six electrons but only at most four (valence) electrons actively participate to the extraordinary properties carbon-based materials feature. Because of the flexibility in

the arrangement of those electrons in sp, sp^2, and sp^3 hybridizations, carbon materials can assume a large variety of allotropic forms with an array of dimensionalities, structure, and physical and chemical properties. For example, recent years have witnessed a continued growth in graphene-based science, in part due to the seemingly bottomless possibilities of arranging carbon atoms into stable structures. While some specific research devoted to graphene will be showcased in this perspective, we emphasize that carbon research is not limited (or even dominated) by graphene-based science. In fact, both *Carbon* and *Carbon Trends* continue to offer an ideal forum to share new findings on more traditional forms of carbon. This is particularly true when new findings, both experimental and/or theoretical, highlight original phenomena that can be translated into applications. For this reason, we continue to strongly encourage the carbon scientific community to not hesitate to revisit old forms of carbon in new disruptive technologies and applications.

This introduction would be incomplete without a mention to how carbon science is positioned in the broader context of the COVID-19 pandemic. As the world is still fighting against the COVID-19 outbreak, scientists from many different fields continue to examine a variety of technological solutions, including carbon-based materials. SARS-CoV-2 belongs to the RNA virus family and has created a medical emergency worldwide due to its lethality and rapid transmission rate. In this context, various carbon nanomaterials (*e.g.,* fullerene, carbon nanotubes, graphene quantum dots, and graphene oxide) have been tested as antiviral substances due to their biocompatibility, relatively low toxicity, and their capability of inhibiting RNA type viruses.[4] Furthermore, significant effort has been devoted to the study of carbon-based biosensors for different types of viruses. There are many challenges: the reproducibility of the material, the control of binding sites, and, in general the reliability and sensitivity of biosensors.[5] Aligned carbon nanotubes have also shown a unique way to enrich viruses that could then be detected via genomic techniques [6] or Raman spectroscopy in conjunction with machine learning [7]. No doubt that more research will continue to help developing methods to assist in tackling the challenges related to the current and (potential) future pandemics.

*Carb*on and *Carbon Trends* Editors have contributed to different aspects of the state of carbon research and crafted a series of editorial sections based on individual subfields.

Conchi Ania describes challenges related to energy conversion and integration of carbon materials in technologies. Alberto Bianco explains the current understanding of biomedical applications using graphene quantum dots and carbon nanodots. Mauricio Terrones describes recent developments on Schwarzites while Chang Liu offers his perspective on carbon nanotube films and fibers. Yuan Chen's contributions addresses the state-of-the-art in ultra-fast heating approach to produce carbon materials. Nikhil Koratkar explains how carbon fibers can be used to develop structural batteries with unprecedented capabilities. Juan Tascon revisits the science of rhombohedral graphite, considering recent developments in this traditional area of carbon research. Yoon Ahm Kim describes recent developments made in the quantification of edges in low-dimensional carbon materials. Finally, Vincent Meunier describes several recent examples of the use of machine learning techniques employed in both computational and experimental studies. Our modest goal is that readers will find these personal opinions and viewpoints helpful.

Energy conversion challenges (COA)

The ambition of developing and deploying clean energy technologies as part of the worlds' climate and clean energy transition policies has created significant pressure on the demand for raw critical materials needed for catalytic reactions for clean energy conversion and climate change mitigation. Some examples include their application to promote oxygen and hydrogen evolution reactions (OER, HER) for water splitting, hydrogen oxidation reaction (HOR), oxygen reduction reaction (ORR) in fuel cells, metal-air batteries, and CO_2 reduction reaction (CO_2RR) for the synthesis of solar fuels and in Li-CO_2 batteries. For example, Pt-based catalysts (typically supported on carbon black) are the most efficient solutions for ORR and HOR, while metal oxides (*e.g.*, RuO_2, IrO_2) are used for OER and HER.[8,9] To alleviate such strains on the demand of critical materials, research efforts are directed towards the development of non-precious metal-based catalysts. Even though some transition metals (*e.g.*, Fe, Co, Ni) complexes have proved to be promising for these reactions, there are still challenges concerning their performance, stability, and long-term operational durability, when compared to commercially available catalysts based on precious metals.[10,11]

Close attention is also being paid on the role of metal-free carbons (MFCs) to replace (noble) metal-based catalysts (Figure 1). Carbon materials have long been used in different catalysts. Interested readers may refer to Section 5 in the last Carbon perspective

published in 2020 for more information. [3] Besides the availability and cost benefits compared to metal catalysts, unique catalytic performance, reusability and stability have been reported for some MFCs in key catalytic reactions for energy conversion and climate change.[12,13] In this context, many metal-free nanostructured carbons have demonstrated excellent ORR performance in alkaline electrolytes, while the efficiency of these materials in acidic electrolytes, which are of interest in polymer electrolyte membrane fuel cells, is still challenging.[14] Metal-free carbon semiconducting photocatalysts have proved to be very appealing for hydrogen generation using solar radiation, their solar-to-hydrogen yields are still lower than those of metal containing catalysts.[15,16]

Another example of energy conversion is in the application of the CO_2 reduction reaction (CO_2RR) for direct conversion of CO_2 into fuels and Li-CO_2 batteries and the nitrogen reduction reaction (NRR) for the synthesis of NH_3 at ambient (T, P) conditions. For CO_2RR, excellent performance has been reported for N-doped carbon catalysts[12,17] in terms of conversion, stability, and selectivity towards CO. Some promising results have been also reported for graphitic carbon nitride-based photocatalysts under sunlight activation.[18] The conversion into more reduced feedstocks (*e.g.,* HCOOH, CH_3OH, C_2H_4, CH_4, CO) using metal-free carbon catalysts still requires further development in order to compete with metal-based electrocatalysts, and promising results on heteroatom-doped diamonds and nanoporous carbons for the production of C1 and C2 products have been recently published.[19,20]

For NRR, current technological challenges are related to the harsh (T and P) conditions of the Haber-Bosch industrial process. Therefore, extensive research is focused on the development of novel processes and more efficient catalysts capable of operating at lower pressure and temperature, and in the separation step. The cleavage of the strong N-N bond is critical in NRR, which is highly dependent on the interaction of nitrogen with the catalyst's surface for subsequent activation. Metal-doped carbons with atomically dispersed metal centers, and the creation of non-electron neutral carbon sites upon heteroatom doping have revealed efficient approaches to achieve high conversions to NH_3 by facilitating the N_2 adsorption while suppressing the competing HER.[21] Tuning of the charge distribution in the carbon framework upon functionalization would seem to be the key to control the conversion of NRR. The immobilization of ionic liquids in the pores of carbon materials has also been reported to increase the uptake of nitrogen gas in carbon

materials with varied porosity.[22] Although no further evidence has been provided about the electrocatalytic activity of such systems, this opens up an interesting possibility for the application of pore-confined ionic liquids in the catalytic activation of nitrogen. The research in this field has progressed significantly, but many challenges remain before the application of carbon-based catalysts for NRR in the production of ammonia can start to compete with the well-established Haber-Bosch process.

Overall, the impact of heteroatom functionalization and the introduction of structural defects on the catalytic activity of CMF catalysts are still quite controversial. The main issues are associated to the unambiguous identification and location of the dopants/defects/active sites of the catalysts, and to a lack of a complete understanding of the catalytic mechanisms. In this regard, recent studies combining experimental and theoretical approaches have addressed these issues on the relationship between catalytic mechanisms, kinetics, and carbon's properties (*e.g.,* defects) to fully exploit the synergistic effects of doping and defects. [14,23,24]

From the application viewpoint, the catalytic active sites for the different energy-related reactions and the optimal operating conditions are usually not the same. For example, most performing OER catalysts work well in neutral/basic conditions, whereas most HER catalysts are only good in acidic medium. Unlike metal-based catalysts, MFCs may present a variety of active sites that can be modulated upon functionalization (*e.g.,* doping, structural defects), enabling multiple catalytic functionalities simultaneously. Such combinations provide attractive approaches for the application of different reactions in self-powered integrated systems, consisting of a photo-electrochemical water-splitting unit and Zn-air battery for renewable generation of electricity from sunlight and water.[13,18,19] A rational design of heteroatom-co-doped porous graphitic networks with interconnected 3D structures has shown that tri-functional catalyst can become efficient at simultaneously catalyzing HER, OER, and ORR in alkaline electrolytes, due to the synergistic effects of the dopants and the 3D porous network.[8] For example, a co-doped MFC catalyst has been developed for the electrochemical overall water-splitting (OER/HER) powered by a Zn–air battery (ORR) using the same catalyst. The integrated units operated in ambient air with a high production rate of hydrogen and oxygen.[19,25] The excellent catalytic activity for the ORR, OER and HER of multifunctional catalysts has been attributed to the effect of heteroatoms on the local charge density distribution of the carbon framework. However, despite the intense research and the promises of building

integrated energy systems, practical applications are still not ready to reach commercial levels.

Challenges in Integrating Carbons in Technology (COA)

Recent years have seen significant progress in the development of novel materials with unexpected properties for a variety of key enabling technologies, such as photonics, nanotechnology, biotechnology, micro/nanoelectronics, energy storage, production and conversion technologies, environment, machine learning, and health. Most innovation research efforts are often based on basic research for optimizing and controlling the materials' properties (*e.g.,* optical, electrical, catalytic activity, etc.), and have produced a large body of scientific publications on record and breakthrough performance for targeted applications.[26–30] Material innovation necessarily involves approaches for a rational design and characterization of such materials, and incorporate tools for predictive materials modelling to control their properties and life cycle performance. Multifunctional materials fulfilling multi-criteria specifications at different scales are desirable and progress in such aspects requires a systematic comparative study of performance offered by other forms (processing or shaping) and architectures of the materials, along with an accurate knowledge of the mechanisms governing the material's properties.

Beyond the incremental progress in carbon materials properties, the integration of innovative materials into structures and systems at technological levels needs to be pursued to validate and fully exploit the breakthroughs observed in materials development. Such applied research is the first step toward the material's practical use in devices, and to boost the technology transfer through the cooperation between research centers and industry.

Attention must be paid to develop adapted processes for the upscale fabrication of such materials (industrial development) and to their integration in large (microscale or macroscale) systems; such integration should be optimized considering the performance at different scales, combining in situ and in-operando characterization of the materials, and boosting devices/processes development for a successful exploitation of the material's functionalities.

The degree of the integration of novel materials at high technological levels depends on the maturity of the target application. Some fields require mainly technological

breakthroughs (*e.g.,* porous carbon adsorbents for water treatment) based on specific operational indicators to evaluate the efficiency of the implementation. Some other sectors (*e.g.,* energy conversion) still need much effort in the development of the devices and testing of the materials in severe conditions (*e.g.,* various loadings, under pressure/in vacuum, at high/cryogenic temperatures, in corrosive atmospheres, etc.).

As an example, the use of porous carbons in wastewater treatment is a mature technology implemented as an end-of-pipe solution in treatment plants. Fundamental research is needed for the development of novel carbon adsorbents for the removal and degradation of pollutants in classic adsorbers or hybrid systems coupling adsorption and advanced process. While classical uptake capacity studies are needed for a first screening of new carbon adsorbents, the best candidates should be investigated in realistic experimental conditions reporting key performance indicators (*e.g.,* carbons density, mechanical properties, particle size, decantability, competitive effects) and key operating conditions (water hardness, organic matter, toxicity, residence time, flow rate, regenerability, reusability). Although these are of paramount importance in process engineering, they are scarcely discussed in the scientific literature.[31–33]

Another example is the increased interest in the application of novel carbons in catalysis (see previous section). Indeed, due to the rapid advance in several fields (*e.g.,* fuel cells, solar fuels production), the market value of carbon materials as substitutes for noble-metal based ones is expected to be triggered in the near future.[34] There are several issues of concern in this field related to data interpretation (nature and distribution of catalytic active sites), comparison of the activity of different catalysts (even for the same authors) and scalability. As the identification of the catalytic active sites of carbon materials is still rather challenging, the comparison of the catalytic activity is usually conducted confronting benchmark materials, or normalizing the activity per (geometrical, porous) surface area or mass. Such practice very often leads to unfair comparisons among catalysts of different nature, as it is the case of most carbons when compared to metallic catalysts.[35,36]

For photocatalytic applications the situation is more complex as commonly defined parameters (*e.g.,* TON, TOF, quantum/photonic efficiency) cannot be easily determined in certain strong light absorbing carbon-based catalysts.[37,38] Thus, it becomes necessary to propose new protocols and descriptors to describe the activity of carbon catalysts following a multiparametric approach considering the joint contribution of

relevant intrinsic properties of the catalyst at a bulk material level, as well as engineering aspects of the reaction (geometry of the reactor, catalyst loading, pressure, residence time, lifecycle, aging, *etc*.).[39–41]

Furthermore, reporting overall catalytic efficiency and performance requires being able to demonstrate the response of the catalysts in the final targeted form (shaping, processability) and considering upscaling aspects. The risks associated with research on novel catalyst are high; materials synthesis' feasibility at laboratory scale and an excellent long-term performance at small scale are not a guarantee that these catalysts can be neither manufactured in a cost-effective way, nor that they will still outperform benchmark catalysts at higher scale. Laboratory scale processing methods should ideally be considered in view of a future upscaling, or at least, basic validation in a relevant environment should be provided. Regrettably, while investigations of fundamental material research aspects are well-described, only very few studies cover engineering aspects of the integration of carbon-based catalysts at relatively large scale.[42–44] Most of the studies report performance on small scale electrodes (typically a few microliters of catalyst ink casted on a few millimeters support), thus extrapolation of their capability to operate in full conditions is not straightforward. Progress beyond materials development urgently needs advances in this direction.

Biomedical engineering of carbon nanodots and graphene quantum dots.

Carbon nanodots (CNDs) and graphene carbon dots (GQDs) have reached in the last years a high popularity within the family of carbon allotropes, with hundreds of publications appearing every month covering a wide range of applications from material science to biomedicine.[45,46] Carbon dots were first identified in 2004 as polyaromatic fragments isolated from the synthesis of single-walled carbon nanotubes (CNTs).[47] They have a size below 10 nm (typically below 5 nm) and a morphology resembling tiny spherical nanoparticles. They are mainly constituted of amorphous and crystalline domains, with the presence of functional groups (*e.g.*, hydroxyl, epoxide, and carboxylic groups, depending on the chemical source for their synthesis) that render them highly soluble. When crystalline structures presenting the typical lattice of graphitic carbon are predominant, they are also identified as carbon quantum dots (CQDs). Graphene quantum dots were described for the first time in 2008.[48] GQDs are zero-dimensional graphene-like structures made of one or few layers with lateral dimensions <10 nm (for an average size of about 5 nm) with high crystallinity associated with the condensed aromatic

carbons.[49] Functional groups are mainly located at the edges, imparting also to these materials a high solubility in all types of organic and aqueous solvents. Since the discovery of CNDs and GQDs, a plethora of methods have been explored for their synthesis covering both bottom-up and top-down approaches. For example, the bottom-up method based on thermal treatment under pressure offers an almost unlimited number of options, as one can burn any type of molecules and combinations thereof to obtain both types of dots. In addition, the possibility of doping such materials with heteroatoms (*e.g.*, nitrogen, sulfur, boron, phosphorous, *etc*.) within their structure allows to tune their physicochemical properties.

Several challenges and limitations of GQDs have been recently reported,[45] and can be equally extended to CNDs or CQDs (Figure 2). One key aspect that is often difficult to characterize is the understanding of the boundary between CNDs, CQDs, and GQDs when simply considering the methods of preparation. In the bottom-up synthetic approach, these three types of carbon nanomaterials can be easily confused. In many publications, the precursors and the protocols are similar, and the authors often categorize the materials using one or the other name. CNDs and GQDs are rather complex, and the variety of structures derives from the choice of their synthesis. Because of the challenge of isolating them and precisely characterizing their structure, it is recommended to use the combination of different analytical (spectroscopic and microscopic) techniques to avoid confusion between the different types of carbon dots. For example, high-resolution Transmission Electron Microscopy (TEM) analysis associated to Energy-dispersive X-ray spectroscopy (EDX) should be applied in a statistical way. Nuclear Magnetic Resonance (NMR) has also been recently proposed as a suitable technique to detect the presence of molecular precursors that generate flaws in the preparation of CNDs when the final materials are not carefully and correctly purified.[50]

The knowledge of the structure of a new material is fundamental in any applications involving therapeutic and imaging uses. The biological responses are valuable, reliable, and reproducible, provided that the materials are carefully synthesized, isolated, thoroughly purified, and characterized. In many publications, there are frequent shortcuts taken in both the preparation and characterization of CNDs and GQDs. Furthermore, the purification protocols and the control of the absence of the precursors are often neglected. In addition, isolation of the dots resides most of the time on a final dialysis. A useful

method to prove the absence of the precursors is the use of high-performance liquid chromatography. It is unlikely that the dots pass through the columns, while small molecular reagents will be easily identified. A careful interpretation of the NMR spectra should also be considered, as one often sees the presence of sharp peaks, that probably correspond to the reagents rather than to the dots which, because they are typically inhomogeneous in size, yield broad bands in the NMR spectra.

In the field of biomedical applications, a mandatory characteristic that these carbon nanomaterials hold is their biocompatibility as limited toxic effects have been reported in most studies.[51] However, more systematic studies on chronic toxicity, possible adverse effects on immune, reproductive and nerve systems are warranted.[52]

GQDs and CNDs are also widely explored for bioimaging. However, in this application there is the challenge of improving the fluorescence quantum yield, which is rather low. To overcome this limitation, the concentrations of CNDs and GQDs used in cell cultures are very high. As the photoluminescence is dependent on particle size, shape, and chemical functionalities, many efforts have been devoted in the last few years to enhance this characteristic. Studies on their optical properties and related mechanisms have shown that they are case-dependent, and very difficult to rationalize.[53]

Another challenge for bioimaging, besides increasing the emission quantum yield, is the need to narrow the fluorescence emission bands to avoid overlapping with other fluorophores for multi-staining. This is a critical limitation in imaging and diagnostic applications. The excitation of CNDs or GQDs often falls into the range covered by the organic dyes or quantum dots used together to stain multiple cellular compartments, leading to possible misinterpretation of the results. For example, most of these materials emit in the green and blue, leading to signals that are affected by high interference and scattering with the tissues. One possibility to overcome this problem has been addressed by developing dots with red or near infrared emission properties. This is still challenging because of the low quantum yield, but holds potential to image deep tissues *in vivo*.[51] Some CNDs have also up-conversion fluorescent properties, that make them good alternatives in bioimaging, as the risk of overlapping in co-staining experiments is negligible.

Interesting features that have been demonstrated for certain CNDs or GQDs are the intrinsic targeting capacity and the specific recognition of intracellular compartments and organelles (*e.g.,* mitochondria, nucleus, endosomes, lysosomes, Golgi apparatus, among others). This presents an encouraging potential for developing such materials to tackle diseases associated to the dysfunctions of the intracellular machinery. CNDs and GQDs are also developed for photothermal and photodynamic therapies in combination with drugs and photosensitizers, respectively. However, these materials are able to produce intrinsically reactive oxygen species, under irradiation, being an alternative to the use of photosensitizers, that often are endowed of undesired toxic effects.[54]

In conclusion, although the development of CNDs or GQDs has grown tremendously over the last few years, there remain many opportunities for improvement. We suggest that future innovation should emphasize the precise choice of precursors, and efforts should be invested to obtain homogenous nanodots with optimal control over their chemical structure. New effective methods to separate the nanodots should also be explored. For example, the use of soft templates in the synthesis would allow to narrow the size distribution and to obtain materials very close to monodispersing and facilitating the elimination of the reagents. Unfortunately, the application of the fundamental advance into industrial use has not reached the same level of interest and maturity of carbon nanotubes and graphene so far. This is likely because there are no standard and well-established methods universally used, as each research group has its own "best" recipe that has led to thousands of materials with their own characteristics. A homogenization and a better control of the synthesis would be a welcome development that would allow for a faster transfer into automatic industrial scaled-up processes. This is also mandatory for registration as new macromolecules/nanomaterials for commercialization. How long GQDs and CNDs will remain at the Lab development? The synthesis, based on using waste or disposals, can be considered green, but sustainability needs to be also demonstrated. The development of CNDs and GQDs has reached a degree of Lab growth that should allow to address the challenges that we have evidenced. Carbon and Carbon Trends journals will consider papers addressing these challenges with great interest.

Schwarzite-inspired carbon composites and beyond

Periodic surfaces appear in different biological systems such as the skeleton of echinoderms, water-lipid surfactant systems, etc. These structures divide the space in interconnected channels that lead to complex surfaces (Figure 3).[55] Theoretically, it has been demonstrated that it is possible to decorate complex labyrinth surfaces with sp^2-hybridized carbon atoms by interconnecting hexagons, heptagons, and octagons (Figure 3).[56–58] These theoretical architectures are mathematically based on triply periodic minimal surfaces (TPMS).[59]

For more than twenty years, it has been very challenging to synthesize these fascinating surfaces with carbon atoms. However, some efforts have shown that it is possible to produce disordered covalently interconnected graphenes and carbon nanotubes exhibiting outstanding properties.[60–62] The challenge ahead is the synthesis of periodic sp^2 carbon surfaces in three dimensions (3D) with periodicities of nanometers. This would require a 3D printer with nanometer resolution, which has not been developed yet. But in the meantime, one could utilize current 3D printers, to print materials (or composites) at the millimeter-centimeter scales and mimic these TPMS to study their mechanical and electronic properties (Figure 4).

For example, some groups have reported superior mechanical properties of 3D polymer networks using 3D printers.[63–65] These systems can be distinguished by their local curvature and the hexagon-heptagon-octagon ratios.[65] These studies have shown that it is possible to combine experiments at the macroscale with molecular dynamics simulations and correlate atomic and macroscopic TPMS.[63,65] The studies indicate that upon deformation, Schwarzite-inspired systems exhibit a unique impact resistance and stress distribution. [65] In addition, these experiments revealed that high strength was proportional to the density of the TPMS and the mechanical properties decrease rapidly when reducing the material's density.[63] Therefore, graphene-decorated TPMS, when synthesized, will offer new materials with properties not seen ever before. From the electronic, chemical, and optical perspectives, these TPMS graphenes will result in materials capable of reversibly storing alkali metals, catalyze reactions (like zeolites) and guide light with different wavelengths, depending on their periodicity and type of TPMS.

As 3D printing of nanometer scale systems is not developed yet, one should think of alternatives to understand the mechanical properties of these TPMS and fabricate

composites with carbon nanomaterials (*e.g.*, nanotubes, graphene) and polymers via 3D printing. These Schwarzite-inspired carbon composites could be a new area in Carbon science, and we encourage our readers to work on these composites to unveil the mysteries of Schwarzites at the macroscale with different nanomaterials embedded.

Single-wall carbon nanotube films and fibers

Single-wall carbon nanotubes (SWCNTs) have a unique one-dimensional tubular structure and excellent physiochemical properties and are therefore expected to have a wide range of important applications. Isolated semiconducting SWCNTs can be aligned to construct micro devices like field-effect transistors where they constitute the channel material of high-performance electronics.[45] However, in general SWCNT-based assemblies including films and fibers are desired for multi-functional uses, since they are structurally strong, flexible, and electrically and thermally conductive.[66] Considerable effort has been devoted to the fabrication of SWCNT films and fibers in recent years, and a key issue is how to translate the intrinsic properties of SWCNTs from the nano- to the macro- scale.

SWCNT films. SWCNTs with a high aspect ratio may connect with each other to form networks, [67] *i.e.*, films. An important potential application of SWCNT films is as transparent electrodes, which should be optically transparent and electrically conductive, and are widely used in various optoelectronic devices including touch screens, liquid crystal displays, organic light-emitting diodes, and photovoltaics. Indium tin oxide (ITO) is currently the most widely used commercial transparent conductive film material because of its good optoelectronic performance. However, ITO is brittle, and the natural reserves of indium are limited. Among the possible alternative transparent conductive materials, SWCNT films are considered very promising due to their excellent flexibility, low intrinsic electrical resistivity, and high structural stability.[68] Nevertheless, the optoelectrical performance of SWCNT films needs to be further improved to reach the level of ITO.

The conductivity of SWCNT films for a given transparency is closely related to their fabrication technique, the structure of the SWCNTs used to assemble the film, the post-fabrication treatment, and the interactions between the nanotubes. SWCNT films can be

prepared by either a wet process or a dry process. For the former, raw SWCNTs are first uniformly dispersed in a solution with the aid of a surfactant, followed by sonication, and centrifugation.[68] SWCNT films are then fabricated by vacuum filtering,[69] spin coating,[70] Langmuir-Blodgett coating,[71] dip coating,[72] spray coating,[73] or Mayer rod coating.[74] In the dry process method, SWCNT films are prepared by the gas-phase infiltration of SWCNTs prepared by a floating catalyst chemical vapor deposition (FCCVD) technique,[75] which involves no liquid. Because contaminants of residue surfactant and defects are inevitably introduced during the dispersion of the SWCNTs, the transparent conductive performance of the SWCNT films obtained by wet processing is usually inferior to that of dry processing. Because SWCNTs usually aggregate into bundles with diameters of tens of nanometers, which decreases the transparency while not contributing much to the electrical conductivity of a film, researchers have tried to make thin films composed of isolated or small-bundle SWCNTs to improve the performance of SWCNT films (Figure 5).[76] Chemical doping has been shown to be a promising way to increase the conductivity of CNT films by improving the concentration of carriers and by decreasing the tunneling barrier between the SWCNTs.[77] Doping with dopants such as H_2SO_4, HNO_3, H_4AuCl, I_2, Br_2, etc. has been shown to improve the conductivity of the films,[68] although a loss of performance over time may occur for these doped samples. Two dimensional SWCNT thin films are comprised of self-assembled CNTs, and there is usually a weak van der Waals interaction between the overlapping CNTs, which leads to a high contact resistance and poor mechanical properties of the films. It has been reported that “carbon welding” efficiently decreases the contact resistance at SWCNT junctions, and hence improves the film conductivity.[76]

A combination of the strategies mentioned above, and newly developed methods are expected to further improve the optoelectrical properties of SWCNT films. From the application perspective, techniques that permit the production of large-area, uniform, high-performance, transparent, and conductive SWCNT films are greatly needed. Various optoelectrical devices fabricated using a SWCNT film as a transparent electrode are expected to emerge and to show intriguing properties. Finally, a CNT film may also be used as a scaffold to construct hybrids/composites making use of their excellent mechanical, optical, electrical, and thermal properties.

SWCNT fibers. Due to the excellent mechanical properties and light weight of SWCNTs, it was proposed that SWCNT fibers would be the only viable candidates for use as the cable of a space elevator,[78] even if many other technological challenges may render the prospect of space elevators very much in doubt. SWCNTs have a very high current carrying capacity of 10^9-10^{10} A/cm^2, which is several orders of magnitude higher than that found in copper. These properties elevate SWCNTs as ideal lightweight, highly stable, and strong conducting wire materials. Individual SWCNTs have diameters of less than 5 nanometers and lengths usually in the micron scale, while assembled SWCNT fibers have a micron-scale diameter and can be prepared in macroscopic lengths. It is particularly desirable that a SWCNT fiber is comprised of well-aligned, densely packed SWCNTs with a high crystallinity, so that the excellent properties of individual nanotubes are translated onto those of the macroscale fibers.

SWCNT fibers can be prepared by self-assembly, gas-phase spinning, and liquid-phase spinning. SWCNT fibers/ropes were initially collected from the products of SWCNTs synthesized by FCCVD[79,80] or arc discharge methods.[81] These samples are self-assembled in the gas flow during the synthesis process and usually have nonuniform lengths and diameters, a low yield, a low packing density, and poor internal alignment of individual SWCNTs. As a result, the mechanical properties of the ropes/fibers are much lower than theoretically predicted.[80,82]. Li *et al.* first reported direct gas-phase spinning of SWCNTs synthesized by FCCVD using a rotating spindle installed at the end of the FCCVD furnace outlet, and fibers were fabricated continuously.[82] Ericson *et al.* dispersed SWCNTs in fuming sulfuric acid to form an aligned phase of individual mobile SWCNTs surrounded by acid anions, then this ordered dispersion was extruded using solution spinning into continuous lengths of macroscopic SWCNT fibers.[83] The gas-phase spinning method presents the advantage that the SWCNTs are directly spun from an aerosol into fibers without experiencing any dispersion and cutting processes. As a result, the SWCNTs retain their initial length, morphology, and structural integrity, which is beneficial to achieve desirable physicochemical properties. However, the technique also presents several disadvantages: the alignment of the SWCNTs is not as good and the packing density is relatively low. As for the liquid-phase spinning method, the SWCNTs can be well aligned using a protrusion process, and the voids between SWCNTs are largely eliminated using a coagulating bath. However, the nanotubes are usually cut short during a dispersion and defects are inevitably introduced into the tube walls.

There are ways to improve the properties of a SWCNT fiber, including using high-quality CNT raw materials, achieving optimized packing of the nanotubes, and establishing a strong interaction between neighboring SWCNTs. Well-crystallized, long SWCNTs have been considered the best candidates for fabricating high-performance CNT fibers, since they have the highest theoretical strength and conductivity. However, recent results have shown that fibers composed of double-wall CNTs (DWCNTs) performed even better.[84] This property is attributed to the fact that the outer shell of a DWCNT protects the inner tube from being destroyed during spinning.

By optimizing the gas-phase spinning, liquid-phase spinning, and post-treatment techniques, well-aligned, densely packed SWCNT fibers with improved properties have been synthesized.[85–87] However, the interaction between the packed SWCNTs is usually weak, which leads to poor stress transfer and a high contact resistance. So, there is still plenty of room to improve the properties of SWCNT fibers by interlinking the nanotubes more efficiently. The strategies described above are expected to lead to the significant improvement of the mechanical, electrical, and thermal properties of SWCNT fibers. This, in turn, will facilitate their applications in ultra-strong and tough fibers and composites, light-weight electrical conducting wires, fibrous energy storage devices and sensors, *etc*.

Carbon material synthesis by ultrafast heating

Carbonization refers to the process of converting carbon-containing solid/liquid/gas precursors into solid carbon materials under heat treatment, usually up to 1500 ^{o}C. Forming graphitic structures above 2500 ^{o}C has been called ‘graphitization’. Standard heating methods used for carbonization/graphitization in conventional furnaces, spray pyrolysis, or solvothermal reactors, are based on thermal radiation, convection, or conduction, in which thermal energy is transferred to carbon-containing precursors, often via media such as a gas or liquid. The heating rate is typically below 100 ^{o}C s^{-1}.

Extensive studies have been carried out to understand carbonization/graphitization under these conditions. The structure and texture of carbon materials strongly depend on the temperature, rate, and duration of the heating procedure, as well as the environment. For example, oxygen and nitrogen start to be released from carbon-containing liquid/solid

precursors from temperatures around 600 °C. Hydrogen would go out from 1000 to 1300 °C, and small and randomly stacked (turbostratic) carbon layers may grow in size with more graphitic regularity above 2500 °C.[69] In comparison, several other heating methods, such as laser irradiation, arc discharging, Joule heating, microwave heating, induction heating, or electron beam radiation, can realize much faster heating rates, *e.g.,* > 10^5 °C s^{-1}. Historically, some fast-heating methods have played critical roles in the discovery of carbon nanomaterials. For example, C_{60} was first found in the soot of laser irradiated graphite.[88] Carbon nanotubes were identified on carbon electrodes heated by the arc discharge.[89]

In the last few years, ultrafast heating methods, especially laser irradiation and Joule heating, have led to a number of developments for the synthesis of new carbon material. When a laser beam irradiates an object, a hot spot is generated where the laser is absorbed. Such a high-temperature hot spot can induce carbonization/graphitization. Laser-induced photothermal effects do not require direct physical contact between heating elements and heated objects, and they can raise temperatures faster than standard heating methods. In 2012, Kaner et al. reported the use of a low-energy infrared laser (788 nm and 5 mW) to irradiate a graphene oxide (GO) thin film (10 μm) (Figure 6a). The heat generated at irradiated spots can quickly reduce the stacked GO film. The laser irradiation method minimizes the restacking of reduced GO (rGO) nanosheets, resulting in porous rGO films with high electrical conductivity of 17.38 S cm^{-1} and a large specific surface area 1520 m^2 g^{-1}.[90] In 2014, Tour *et al*. accidentally found that the irradiation by a high-power CO_2 laser (10.6 μm, 2.4–5.4 W) can convert a polyimide film (127 μm) into carbon materials containing randomly stacked graphene layers with an electrical conductivity of 5–25 S cm^{-1} and specific surface area of 340 m^2 g^{-1}, which is significantly different from glassy carbon, the common carbonization (at 800–1500 °C) product of polyimide (Figure 6b). A threshold laser power is required to initiate the graphitization process. It was proposed that laser irradiation could create high localized temperatures (> 2500 °C), which drive out nitrogen and oxygen from polyimide. Aromatic and imide repeat units in polyimide are essential for the formation of graphitic structures.[91] Further studies have revealed that the porosity, composition, morphology, and surface chemistry-related properties (*e.g.*, superhydrophilicity and superhydrophobicity) of carbon materials could be further engineered by adjusting laser parameters, atmosphere, and substrates or introducing additives to precursors.[92] A wide range of precursors without aromatic and

imide repeat units can also be graphitized in two laser irradiation steps. The precursor is converted into amorphous carbon during the first laser irradiation, followed by graphitization under a second laser irradiation at higher temperatures.[93] Notably, a unique advantage of laser irradiation methods is their capability of selectively creating micrometer-scale patterns under ambient conditions. In this case, the size of laser spots limits the resolution. 3D structures can also be made by combining laser irradiation with the physical assembly of multiple 2D layers.[94]

Joule heating refers to the conversion of electrical energy to heat when an electrical current flows through a conductor. Joule heating has been widely used in conventional furnaces, for example, graphite furnaces in industrial graphitization processes. In 2016, Hu et al. reported that adjacent carbon nanofibers (CNFs) derived from polyacrylonitrile can be welded together by Joule heating CNF film at a high temperature (>2227 ^{o}C). The welded CNF film shows an electrical conductivity of 380 S cm^{-1}.[95] The same method was also applied to achieve fast annealing of rGO film (4 μm in thickness) at (2477 ^{o}C), resulting in a high electrical conductivity of 3112 S cm^{-1}.[96] These two studies proposed that Joule heating can efficiently remove defects and other functional groups from original carbon structures,[97] facilitate better linkage/bridging among neighboring carbon nanostructures (*e.g.*, CNFs or rGO nanosheets), leading to continuous 3D carbon networks. Gao et al. developed this method into a high-throughput roll-to-roll process (Figure 6c) to fabricate flexible rGO films with the electrical conductivity of 4200 S cm^{-1} and thermal conductivity of 1285 W m^{-1}K^{-1}.[98] Using Joule heated rGO or CNF films as fast heating and cooling platform to control the nucleation and aggregation of different elements, metal nanoparticles,[96] multi-metallic alloy nanoparticles,[99] single metal atom catalysts,[100] and ceramics[101] have been synthesized for various applications.

In 2020, Tour *et al*. reported a new Joule heating process, in which a large capacitor bank quickly delivers electrical energy to conductive and amorphous solid carbon powder loosely packed inside a quartz tube (Figure 6d), bringing the temperature higher than 2727 ^{o}C in less than 100 ms and releasing gases through the gap.[102] Using this method, bulk carbon materials with a yield of 80 to 90% were obtained from carbon black, which have a specific surface area of 295 m^{2} g^{-1} and contain small graphene sheets (13 nm in size) in a turbostratic arrangement. They are more oxidatively stable than rGO obtained from the Hummers' method. Carbon material structures derived from the Joule heating process

depend on process parameters and carbon precursor compositions.[103,104] For example, carbon materials derived from coffee grounds or anthracite coal contain larger graphene sheets with an average size of 0.5 and 1.2 μm, respectively. A short healing period of 30–100 ms is critical to prevent the stacking of turbostratic graphene layers into bulk graphite.[105] Using organic fluorine compounds and fluoride precursors, different carbon allotropes, including fluorinated nanodiamonds, fluorinated turbostratic graphene, and fluorinated concentric carbon, have also been synthesized.[106]

These new developments show that ultrafast heating can produce new material structures and textures. Carbon materials produced by ultrafast heating methods often have fewer defects, more uniform crystalline structures, and more continuous 3D networks. They are also more oxidation resistive with higher electrical conductivity. Future research efforts are needed to understand the relationship between ultrafast heating parameters and short-range and long-range orders in carbon materials. These efforts will broaden the application potential of these carbon materials. It may also bring improvement for existing carbonization/graphitization processes.

Carbon-Fibers for Next-Generation Structural Batteries

Housing rechargeable batteries in electric mobility applications involves the use of dead-weights that can severely affect the range and time of operation.[107] A compelling solution to this problem is the integration of batteries as both power sources and structural parts of vehicles with mechanical load-bearing capability. This idea of "structural battery" or "mass-less energy storage", has attracted the attention of researchers and leading automobile manufacturers alike.[108] In this context, carbon fibers (CFs) consisting of more than 90% pure carbon, and which are traditionally used as reinforcements in structural composites, are of great interest because of their exceptional multi-functionality. Like graphite, CFs also have low lithium insertion potential, which makes them a favorable anode material for structural lithium-ion batteries (SLIBs).

A typical CF structure consists of graphene planes that are mis-oriented with respect to each other and contains defects.[109] As a result, their lithium insertion mechanism closely resembles to that of disordered carbons in which defects provide additional lithium storage sites.[110] Between pitch-based and polyacrylonitrile (PAN)-based CFs,

the latter shows better charge storage capacity because of higher disordering in the carbon structure.[111] Nevertheless, initial SLIB prototypes based on CFs have not delivered satisfactory performance, possibly due to poor electrical insulation, fewer solid electrolyte candidates, lack of compatibility, and absence of scalable manufacturing processes. While there is no standard design for SLIBs, many of the previous works have revolved around either laminated type (more common) or 3D-fiber type SLIBs (Figure 7).

As these designs[112–115] feature CFs embedded inside the electrolyte matrix, it is important to understand the effect of lithiation of CFs and its impact on the battery composite. Jacques *et al.* observed that the ultimate tensile strength drops by 20 to 30% when the CF anode is fully lithiated and is only recovered partially during delithiation.[116] This indicates that some lithium gets trapped in the turbostratic structure of CF during delithiation. Recently, Duan *et al* used corrosion protected carbon fibers to demonstrate that the transverse modulus of lithiated CF is nearly twice as large as that of either pristine or delithiated CF.[117] This increase is attributed to stiffening of the out-of-plane (C_{33}) and shear (C_{44}) elastic constants. In addition, a softening effect is observed for longitudinal modulus after lithiation, which is like the softening effect of the in-plane (C_{11}) elastic constant of graphite. Despite this longitudinal softening, the impact of lithium insertion does not appear to be a significant impediment to the utilization of CFs in structural battery development.

A key driver to improving SLIB performance is the design of the electrolyte. An ideal structural battery electrolyte should have high ionic conductivity (> 0.1 mS cm^{-1}) and it should form an intimate contact with CFs such that mechanical load and ions can transfer between the fibers and electrolyte matrix. Solid polymer or gel polymer electrolytes (SPE or GPE) are usually preferred due to their semi-solid nature; however, a trade-off is commonly observed between stiffness and ionic conductivity. A bi-continuous polymer electrolyte, developed recently via reaction-induced phase separation, showcased a high stiffness of 0.5 GPa and conductivity of 0.2 mS cm^{-1}.[118] Very recently, Asp *et al* employed IMS65 CF and similar electrolyte, to design a laminated structural battery composite with energy density of 24 Wh kg^{-1} and elastic modulus of 25 GPa.[119] This design, which consists of multifunctional components, surpasses previous structural battery reports that prioritized either electrical or mechanical properties. Another

promising design consists of carbon fiber tow (~1000 CFs) surrounded by a polymer matrix coating that is in contact with a lithium iron phosphate electrode and an aluminum current collector.[114] Unfortunately, this SLIB while promising showed a low-capacity retention, especially with increasing CF content per tow.

While significant progress has been made to date, there is still a long way to go before SLIB technology can be implemented in practice. Combining new designs that can improve the overall structural performance, along with other strategies such as building stronger constituent materials, while simultaneously developing advanced material chemistries, will be necessary to move SLIB technology forward. If this can be achieved, then the ramifications can be immense, especially for transportation applications. While the automotive industry (*e.g.,* electric vehicles) will benefit greatly, the impact of this technology can be particularly transformative on the aerospace industry. Structural weight is at a premium in both manned and unmanned aerospace vehicles including fixed-wing aircraft and helicopters. Unless the battery is fully integrated into the structure and is the primary load bearing element, it is difficult to visualize how electrification of aerospace vehicles can become a reality. SLIB technology therefore seems to hold the key to enabling the next generation of all-electric aircraft.

Rhombohedral Graphite

There are two possible types of graphene layer stacking in natural graphite: hexagonal, Bernal type (ABA sequence) and rhombohedral (ABC sequence). They are shown in Figure 8 together with a third hypothetical stacking (*i.e.*, simple hexagonal, AAA sequence). These structures differ in the horizontal shift imposed on the middle plane in the ABA-stacking, on all planes in the ABC-stacking, while all the planes are directly above each other in the AAA-stacking. The rhombohedral structure is metastable and transforms to the hexagonal structure upon heating above 1300 ºC. For this reason, it is generally considered that it cannot be found in synthetic graphites obtained by heat treatment. Furthermore, attempts to prepare pure rhombohedral graphite have hitherto failed. Therefore, very little knowledge is available about this form of graphite compared with the hexagonal form. In fact, in view of the minor importance of rhombohedral graphite, the IUPAC terminology norms explicitly tolerate the use of the term “graphite” instead of the more accurate term “hexagonal graphite”.[120] We present here an

overview of salient facts concerning rhombohedral graphite with some focus on recent results obtained with trilayer graphene and also on recent results from the van der Waals technology, which has made it possible to produce high-quality rhombohedral graphite films up to a thickness of 50 layers of graphene, offering a promising way to tailor graphitic materials with novel properties.

Following seminal reports on the structure of graphite, [121–123] the existence of rhombohedral graphite was first documented by Lipson and Stokes.[124,125] In the 1950s, several authors [126–129] contributed further crystallographic data to characterize this graphite-type structure and/or reported on the effects of mechanical stress, exposure to high pressure, and high temperature treatments on the proportions of rhombohedral *versus* Bernal's hexagonal forms. Later, Gasparoux modified the magnetic properties of graphite by means of a moderate grinding carried out with the objective of creating rhombohedral sequences.[130] Alternatively, the variation of the magnetic susceptibility with high temperature treatment provided information on the transformation of the rhombohedral structure into hexagonal. Wilhelm *et al.* [131] also studied the formation of rhombohedral sequences and developed a model to describe the interstratification of the hexagonal and rhombohedral forms. Based on these and other works, the structure of rhombohedral graphite has been considered as an extended stacking fault in hexagonal graphite.[120]

With regard to theoretical works, the band structure and electronic properties of rhombohedral graphite were first investigated using the nearest-neighbor tight-binding approximation.[132,133] Charlier *et al*. [134] examined the effect of graphene stacking on the electronic properties of graphite in a first-principles study. They considered the Bernal and rhombohedral structures, in addition to the hypothetical "simple hexagonal" graphite with an AAA stacking sequence shown in Figure 8. Band structure and density of states results indicate that these three allotropic forms of graphite possess a semi-metallic behavior with the overlap between conduction and valence bands depending on the stacking position of graphene sheets. More recently, Dadsetani *et al*.[135] computationally studied the near-edge structure of rhombohedral graphite and several other carbon allotropes within the density functional theory (DFT) approach. The main objective of that work was to interpret data reported for "n-diamond", a new phase that

certain authors considered as a possible intermediate between rhombohedral graphite and diamond. [136]

Several experimental works over the last two decades have reported on application of new characterization techniques and/or finding of rhombohedral graphite in a variety of products, for example exfoliated graphite flakes,[137] or graphite blocks produced from natural graphite flake.[138] In the latter, isolated rhombohedral crystallites with homogeneous ABC stacking were detected for the first time in graphite blocks in addition to mosaic distributions of the rhombohedral phase in a hexagonal host (previously, the rhombohedral structure was widely considered as a mosaic that was produced only by mechanical shear or milling). Roviglione and Hermida [139] found a large amount of rhombohedral graphite in spherical carbon particles (nodules) extracted from a ductile iron matrix. According to the authors, this can only be attributed to plastic deformations produced during the growth of the nodules from the melt, and formation of the rhombohedral phase is the response of graphite to the large requirements of out of equilibrium conditions. Ortiz-Morales *et al*. [140] reported the finding of rhombohedral graphite (mixed with hexagonal graphite and residues of Ni, Fe and Co catalysts) in single-wall carbon nanotubes synthesized by hydrogen-arc-discharge.

The advent of graphene has sparked increased interest in few-layer graphene materials, of which trilayer graphene is particularly relevant due to the clear differences in properties between ABA or ABC stacking configurations. Pierucci *et al.* [141] synthesized large-area uniform trilayer graphene (consisting of large and flat domains) on SiC. They used photoemission spectroscopy and scanning tunneling microscopy/spectroscopy to examine the electronic structure of ABA and ABC trilayer graphene and compared it to DFT calculations. Their findings demonstrate a pronounced effect of stacking order and charge transfer on the electronic structure of trilayer or few-layer graphene. Zhang *et al*. [142] found that ABA and ABC stacking, which are very common in few-layer graphene, can be well distinguished by whether their highest-frequency shear modes are observed in their Raman spectra at room temperature. In fact, as Figure 9 shows, they can be observed in N-layer graphene (NLG, N = 3, 4, 5, 6) with ABA stacking (denoted by the authors as “AB” in Figure 9), but not in the case of ABC stacking. Consequently, as proposed in a number of other studies as well,[143] these authors proposed Raman

spectroscopy as a method to characterize the stacking order in these and other two-dimensional layer materials.

Recently, Latychevskaia *et al.* [144] have demonstrated two possible ways to controllably and locally transform the ABC stacking in few-layer graphene into the ABA stacking. One method proceeds using Joule heating and the transition between the two phases is characterized by monitoring the 2D peak in the Raman spectra. In a second approach, the transition was achieved by heating through illumination of the ABC region with laser pulses, and the transition was visualized by TEM. The first method allows starting the transition with a spatial resolution of about 1 μm, while the second method allows triggering the transition of larger areas (20–40 μm, depending on laser intensity). No evidence for diamond formation was obtained in either case.

Yang *et al* [145] have demonstrated an efficient strategy to control the stacking order of graphene layers in graphite using the van der Waals heterostructure technology.[146] This technology consists of layer-by-layer assembling of different one atom-thick structures, thus yielding materials that exhibit strong bonding within each individual layer and weak bonding between layers. This has resulted in high-quality rhombohedral graphite films up to 50 graphene layers thick.[147] The authors performed a directional encapsulation of ABC-rich graphite crystallites with hexagonal boron nitride (hBN) and found that this encapsulation, which is introduced parallel to the zigzag edges of graphite, preserves the ABC stacking, while the encapsulation along the armchair edges transforms the stacking to ABA. As Figure 10a illustrates (using ABC trilayer as an example), a shear force applied to graphite leads to a displacement of the graphene planes in a “stick−slip” fashion. If the displacement occurs along zigzag edge directions, it will preserve the stacking order, while displacement parallel to armchair edges will alternate stacking order between ABA and ABC. The encapsulation protocol for ABC-stacked graphite was modified with the goal of significantly increasing the chance of the survival of this energetically less stable stacking allotrope. To do this, the authors used the polydimethylsiloxane (PDMS) transfer technique, in which this viscoelastic polymer allows precise control of the contact area between the poly(methyl methacrylate) (PMMA) adlayer and the substrate (Figure 10b). This research was carried out with the aim of investigating the fascinating, electronic properties for ABC-stacked graphite that have been theoretically predicted (see Ref. [145] and references therein), as prior to this

there were no experimental results on electron transport in ABC-stacked graphite films thicker than tri- or tetralayer. In a subsequent work, the same team studied the electronic transport behavior of the obtained high-quality multilayer graphene films and showed a pronounced hysteresis and other characteristic signatures of electronic phase separation, which have been attributed to the appearance of strongly correlated electronic surface states.[147]

Finally, we wish to emphasize that this section is titled "rhombohedral graphite" rather than "rhombohedral carbon". Rhombohedral symmetry occurs in some non-sp^2 carbon solids, which are deliberately excluded from this brief account for the sake of homogeneity. This is, for example, the case of a C_{60} rhombohedral phase, which has been found both theoretically [148] and experimentally,[149] as well as several rhombohedral ultrahard carbon phases that resemble diamond more than graphite. Thus, a new ultrahard rhombohedral carbon polymorph whose structure is very close to diamond's has been found in impacted meteorites.[150] A simulation of the structural transformation of rhombohedral graphite-like carbon into three-dimensional dense forms has recently been performed by geometry-optimization calculations within DFT. The resulting rhombohedral solids, rh-C2 [151] and rh-C4,[152] have been predicted to possess slightly better mechanical properties than diamond and lonsdaleite.

Quantifying Edges in Low-dimensional Carbon Materials

In reduced dimensions, carbon materials consist of two different types of surfaces: the basal and edge planes. The basal plane is homogeneous and composed of only carbon atoms, whereas the edge plane is heterogeneous and terminated by passivating atoms and groups of atoms such as hydrogen and oxygen functional groups. Generally, it is the edge plane that makes the most significant contributions to the electronic and chemical properties of carbon materials. For example, the edge plane has much higher electrocatalytic activity and oxidation reactivity than the basal plane. The edge sites in carbon materials are closely related to side reactions, such as corrosion, gas evolution and formation of a solid electrolyte interphase layer. The edge plane also acts as the main reactive sites of doping and functionalization because the functional groups or heteroatoms can be more easily attached to chemically active edge sites than the basal plane. However, although the importance of the edge plane has been established qualitatively thus far, a limited number of studies have been reported on the effect of edge

density on the physicochemical properties of carbon materials. Therefore, many efforts continue to be made to develop analytical tools to measure the edge plane quantitatively to understand surface properties of carbon materials.

In 1960, the concept of active surface area was developed to evaluate the number of active sites by measuring the amount of chemisorbed oxygen around 300°C.[153] Although this concept is highly helpful in understanding the carbon-oxygen gasification reactivity, the active surface area has no direct relationship with the carbon edges. The second method involves estimation of the number of edge sites, basal planes and defect sites using their different adsorption energies from nitrogen adsorption data. [154] However, the accuracy of this approach is limited and is only applicable to graphite.

A recently developed method to measure the number of active sites, the high temperature programmed desorption (TPD) (up to 1800 °C), allows a quantitative evaluation of edges with high accuracy through measurement of evolved gases.[155,156] Since the edge sites in carbon materials are usually terminated by hydrogen or oxygen functional groups, they typically decompose to H_2, H_2O, CO and CO_2 below 1800 °C (Figure 11a), and the number and surface area of those sites can be calculated from deconvoluted TPD profiles (Figure 11b). It is assumed that H_2 is released from the reaction between two C-H bonds, while H_2O is generated due to reaction between a C-H bond and a hydroxyl group. The number of hydrogen atoms that are terminated at the edge sites, N_H, has been calculated from two H_2 and one H_2O.[157] Additionally, the anhydride and the lactone groups were counted as two edge sites from their functional group structures. From these assumptions, the number of edge sites, N_{edge}, can be calculated as follows:

$$N_{edge} = N_H + Carboxylic^{TPD} + 2{\cdot}Anhydride^{TPD} + 2{\cdot}Lactone^{TPD} + Phenol^{TPD} + Ether^{TPD} + Carbonyl^{TPD}$$

Using the number of edge sites, the surface area of the edge sites, S_{edge}, can be further calculated using the area assigned to each carbon atom from:

$$S_{edge} = N_{edge} \times A_{edge} \times N_A$$

where A_{edge} = 0.083 nm^2 is the calculated average area of each carbon atom, and N_A = 6.022×10^{23} mol^{-1}.

Based on the application of the TPD method on edge-enriched carbon nanofibers (CNFs) as a model compound, it can be inferred that the edge density is directly related to the electrocatalytic performance of carbon materials.[158] The edges on the surface of the CNFs were physically passivated by forming loops between adjacent edges using high-temperature thermal treatment. The physically passivated CNFs were then chemically inactivated with amine groups via amination reaction. Finally, it was verified that the hydrogen evolution reaction was directly related to the number of active edge sites in the CNFs (Figure 11c). Furthermore, the edge sites can act as corrosion reactive sites in electrochemical applications of carbon materials.[159] In addition, tailored porous carbon with a small number of edges can be used to fabricate powerful and durable energy storage devices under extreme operating conditions.[160,161]

Although the importance of edge planes in carbon materials has been intensively studied for the last 40 years, their full potential could not be realized to-date. This is mainly because of the following reasons: (1) the edge configuration changes continuously due to chemical functionalization, (2) although the quantitative tool for measuring the edges in carbon materials has been established, there is no characterization method to evaluate the spatial distribution of edges on the surface of the carbon materials, and (3) there is no simple way to create specific types of clean and stable edges in a controllable fashion. Therefore, more advanced characterization tools should be developed which can accurately measure the density and the type of edges, and their spatial distribution on the surface of the carbon materials.

Machine Learning in Carbon Research

The popularity in the use of materials informatics continues the sharp increase we already noted in the 2020 Carbon perspective article. Materials informatics encompass a broader and broader range of applications, such as the management of big data, high-throughput computational investigations, and the use of artificial intelligence (AI) methods. The sustained growth in this field is intimately linked to the availability of increasingly accurate theoretical descriptions of materials properties and to the continuous development of supercomputing power accessible, at a modest cost, to a larger and larger number of researchers. This availability is now allowing huge advances in materials data science and, specifically, machine learning (ML) techniques. ML consists in the application of mathematical principles and computer algorithms that aim at improving

performance (*i.e.,* predictable power) based on the training performed on well-established data. In carbon research, we are clearly at a crossroad where broadly two types of research now proceed in parallel: on one hand, algorithms and computational techniques continue to be developed at a high rate by computer scientists and applied mathematicians and, on the other hand, materials engineers and scientists are *users* of those algorithms as they become available in the form of open-source libraries, often in the Python programming language. In this context, it is not surprising that the Editors of *Carbon* and *Carbon Trends* keep receiving a growing number of original article submissions on this topic and we strongly encourage authors to use our journals to disseminate their work in this area.

A large portion of recently reported studies deals with machine learning algorithms using computational data as learning dataset. However, the portion of ML studies related to the treatment of experimental data has been growing steadily, as ML algorithms are becoming more and more available to the broad community. The goals of both types of investigation are the same: using a subset of well-understood data to develop predictive models applied to systems that are difficult to treat explicitly.

Machine learning and computed data: Several ML studies have been devoted to understanding nanomechanical properties. For instance, shallow neural networks were used to predict the fracture stress in defective graphene, including parameters such as temperature, vacancy concentration, strain rate, and loading direction. Data required to model Convolutional Neural Networks (CNNs) were obtained from molecular dynamics (MD) simulations. [162] In a separate study, a deep learning framework was built using tensile tests performed by MD at room temperature on SWCNTs up to 4 nm in diameter. An artificial neural network was trained using the MD dataset and subsequently used to predict the mechanical properties with high fidelity. [163] Likewise, h-BC_2N lattices were investigated using theoretical models based on machine-learning interatomic potentials (MLIPs) to explore the mechanical/failure and heat transport properties under ambient conditions. [164] In general, studies have shown that the use of MLIPs can significantly reduce computational costs while achieving accuracy close to that of *ab initio* methods. MLIPs are trained on large datasets obtained from *ab initio* calculations. For instance, a deep learning approach was used to train neural network potentials (NNPs) using the CA-9 dataset, (made up of results obtained for 9 carbon allotropes) to accurately reproduce structural and vibrational properties, with accuracy similar to that of DFT.

[165] Passively-trained MLIPs were also employed to study thermal expansion of several carbon-based nanosheets. MLIPs were found to be very accurate at reproducing DFT phonon properties.[166] In addition, the thermoelectric performance of g-graphyne nanoribbons (g-GYNRs) was optimized using a combination of nonequilibrium Green's function and Bayesian optimization, showing that Bayesian optimization can accurately identify the optimal structure with best thermoelectric efficiency, identifying room-temperature figure of merit of optimal defective g-GYNR as high as 2.315, which is 5 times of that of pristine g-GYNR. [167] Stochastic *ab initio* random structure search algorithm was combined with the use of interatomic potentials to predict the structure of a large dataset of carbon clusters spanning a wide range of sizes (Figure 12). The study is particularly illuminating as the researchers systematically compared the transferability and predictive capability of seven popular carbon potentials, including classical and machine-learning potentials, finding that the GAP-20 potential [168] is the most accurate at predicting the properties of carbon clusters. [169]

Machine learning has been used in several studies where the computed vibrational properties of a carbon sample are employed to determine the underlying structure. For instance, in a study focused on point vacancies in a carbon nanotube. a polynomial support vector machine (SVM) was developed to successfully classify pristine and (vacancy) defective SWCNTs at test accuracy greater than 90%. [170] In another research, a machine learning-based approach was developed to provide a continuous model between the twist angle and the simulated Raman spectra of twisted bilayer graphene (tBLG). Once trained, the machine learning regressors (MLRs) quickly provide predictions without human bias and with an average 98% of the data variance being explained by the model. [171] Evolutionary algorithms can also be used for crystal structure prediction, such as stable two-dimensional (2D) carbon allotropes. For instance PAI (polymerized as-indacenes) graphene was predicted as a stable 2D allotrope of graphene using these types of techniques. [172]

Carbon researchers also exploit machine learning techniques to develop new interatomic potentials that are both accurate and transferrable. [168,173,174] For example, a geometry-driven deep learning framework Geometry Orbital of Deep Learning (GOODLE) was recently developed to accurately predict carbon properties in both real and reciprocal spaces. These properties include energy, equation of states, phonon

structure, electronic band structure, and optical absorption. GOODLE is trained on small lattice carbon structures and was found to be capable of accurately describing an array of structures, including magic-angle tBLG. [175]

Machine learning and experiment: Moving to recent studies involving experimental characterization and synthesis techniques, a Convolutional Neural Network was developed to assist in the tedious determination of chiral indices in CNTs, based on the analysis of high-resolution transmission electron microscopy (HRTEM) images. This approach allows the analysis of a large number of HRTEM images of carbon nanotubes, leading to predictive estimates of experimental chiral distributions.[176] In another study, Raman spectroscopy was used to understand the structural development that occurred in the biomasses during pyrolysis. A multivariate analysis based on the combined Principal Component Analysis, partial least square-discriminant analysis (PLS-DA) was employed for the Raman data to classify biomass with respect to their source and activation temperature. Deep learning methods (*e.g.,* LeNET, ResNet, CAE) were evaluated to classify the bio-carbon samples with respect to temperature and precursor material, yielding excellent classification with respect to the temperature of activation. [177]

Another study was reported on the optimization of the yield of CVD-grown single-wall carbon nanotubes under the constraint of minimizing the tube diameter. A total of eight process parameters were considered in the constrained optimization. Then, an artificial neural network (ANN) coupled with a Taguchi analysis was able to highlight the interplay between process parameters. This approach features a 90% accuracy, showing that furnace temperature primarily affects the diameter, whereas, methane flow-rate determines the yield. [178] The optimization of laser-induced graphene (LIG) is also time-consuming and expensive. For this reason, an automated parameter tuning technique based on Bayesian optimization was developed for the rapid single-step laser patterning and structuring capabilities with the goal of facilitating the fabrication of graphene-based electronic devices. Experimental parameters that were optimized include laser power, irradiation time, pressure, and type of gas. [179] Carbon fiber manufacturing is a complex activity as it involves up to 70 processing variables. ML models (*e.g.,* vector regression (SVR), multi-layered perceptron (MLP) neural network, gradient boosted regression trees (GBRT), and recurrent neural network (RNN)) are particularly well suited for the optimization of such a parameter space. Those techniques were used to map precursor

information and carbonization process parameters to mechanical properties, using an experimental dataset of 600 distinct points with 31 features. The results indicate that ML can be used to approximate the underlying function describing the effect of the manufacturing process parameters on the carbon fiber tensile properties, with the RNN model outperforming all other models under consideration [180]

Finally, we note that ML can also be used to optimize energy applications of carbon materials. For instance, insight into understanding hydrogen uptake in porous carbon materials can be gained from the development of machine learning models, and, in turn, could lead to the rational design of materials with optimal hydrogen storage. For example, random forest was used on a dataset containing 68 different experimental samples and 1745 data points, along with an analysis based on Shapley Additive Explanations (SHAP). The analysis indicated that pressure and Brunauer-Emmett-Teller (BET) surface area are the two strongest predictors of excess hydrogen uptake. Strikingly, a positive correlation was also found with oxygen content. The pore size distribution is also found to be important, since ultramicropores (size below < 0.7 nm) are found to be more positively correlated with excess uptake than micropores (size below < 2 nm). [181]

It is expected that despite the growing popularity of ML techniques in the Carbon community, the field is still largely in its infancy, and we anticipate that ML techniques will become mainstream in synthesis, characterization, and device development within the next few years. The availability of advanced ML techniques and the relative ease to deploy them efficiently will continue to drive the tremendous progress in this area and will continue to pave the way to discoveries. However, to harness the full potential of materials informatics will require sustained efforts in the development of broadly adopted approaches to data storage, curating, and analysis.

Conclusions and perspectives

This perspective has summarized some of the most impactful carbon research developed worldwide over the past couple of years and emphasizes the challenges that lie right ahead. Innovation in carbon materials' science must move beyond the incremental progress in new design methods. For instance, advances towards the integration of new carbon materials with promising features at higher technological levels are needed to validate the performance at large scales. This is particularly critical given the fact

materials synthesis' feasibility and performance at small scale are not a guarantee for reproducible upscaling. Furthermore, most research efforts cover fundamental material research aspects and the extrapolation of materials' capability to operate in relevant environments is not straightforward from small scale laboratory tests. Nontraditional processing methods (*e.g.*, Joule heating, laser heating, van der Waals heterostructure technology…) are continuously contributing to the synthesis of novel forms of carbon. Perhaps more important, they are expected to provide efficient ways to finely tailor carbon materials structure and texture according to future needs. Creating novel carbon structures relies on suitable chemical precursors and carbonization/graphitization conditions. Although heating conditions have been studied for many years, recent developments in ultrafast heating methods show the formation of new carbon material structures and textures. Understanding the precise control of these methods will open the opportunities to create a wide range of novel carbon materials. These materials will find application opportunities in catalysis, energy storage, waste management, construction, smart systems, etc. SWCNT films and fibers have shown appealing optoelectrical, electrical, thermal, and mechanical properties, in addition to their light weight and desirable chemical stability, these macroscopic nanotube assemblies are expected to find applications in a wide range of areas. Finally, recent advances have clearly indicated the major role that machine learning approaches will play in the foreseeable future in both the treatment or large-data and the optimization of synthesis/processing methods. We anticipate seeing a sharp increase in publications involving ML in *Carbon* and *Carbon Trends*.

Both journals *Carbon* and *Carbon Trends* keep receiving more manuscripts every year. Our editorial teams are devoted to research novelty and encourage authors to submit manuscripts reporting breakthroughs and significant advances in many subfields of carbon research, including those described in this document. *Carbon* and *Carbon Trends*' mission is to continue to publish cutting edge research (both fundamental and applied, encompassing the physics, chemistry, engineering, and biophysics aspects of carbon). Based on our experience with the review process, we encourage submission of computational works performed in tandem with experiment directly to *Carbon* but, at the same time, we suggest that purely computational and theoretical works (including ML based research) be submitted to *Carbon Trends*, as one of our new journal's objectives is to become a medium of choice to share this type of reports.

Acknowledgements

Y.A.K. acknowledges the financial support from the National Research Foundation of Korea (NRF) grant funded by the Korea government (MSIP) (No. 2021R1I1A305628711). A.B. gratefully acknowledges the Centre National de la Recherche Scientifique (CNRS) and the International Center for Frontier Research in Chemistry (icFRC) (Strasbourg, France). J.M.D.T. acknowledges joint partial funding from Gobierno del Principado de Asturias and European Regional Development Fund (ERDF/FEDER) (grant IDI/2021/000037). Y.C. acknowledges the financial support from the Australian Research Council under the ARC research hub for safe and reliable energy (IH200100035).

References

[1] J. Zhang, M. Terrones, C.R. Park, R. Mukherjee, M. Monthioux, N. Koratkar, Y.S. Kim, R. Hurt, E. Frackowiak, T. Enoki, Y. Chen, Y. Chen, A. Bianco, Carbon science in 2016: Status, challenges and perspectives, Carbon N. Y. 98 (2016) 708–732. https://doi.org/10.1016/j.carbon.2015.11.060.

[2] A. Bianco, Y. Chen, Y. Chen, D. Ghoshal, R.H. Hurt, Y.A. Kim, N. Koratkar, V. Meunier, M. Terrones, A carbon science perspective in 2018: Current achievements and future challenges, Carbon N. Y. 132 (2018) 785–801. https://doi.org/10.1016/j.carbon.2018.02.058.

[3] A. Bianco, Y. Chen, E. Frackowiak, M. Holzinger, N. Koratkar, V. Meunier, S. Mikhailovsky, M. Strano, J.M.D. Tascon, M. Terrones, Carbon science perspective in 2020: Current research and future challenges, Carbon N. Y. 161 (2020) 373–391. https://doi.org/10.1016/j.carbon.2020.01.055.

[4] J. Sengupta, C.M. Hussain, Carbon nanomaterials to combat virus: A perspective in view of COVID-19, Carbon Trends. 2 (2021) 100019. https://doi.org/10.1016/j.cartre.2020.100019.

[5] J. Sengupta, C.M. Hussain, Graphene-based field-effect transistor biosensors for the rapid detection and analysis of viruses: A perspective in view of COVID-19, Carbon Trends. 2 (2021) 100011. https://doi.org/10.1016/j.cartre.2020.100011.

[6] Y.T. Yeh, Y. Tang, A. Sebastian, A. Dasgupta, N. Perea-Lopez, I. Albert, H. Lu, M. Terrones, S.Y. Zheng, Tunable and label-free virus enrichment for ultrasensitive virus detection using carbon nanotube arrays, Sci. Adv. 2 (2016). https://doi.org/10.1126/sciadv.1601026.

[7] Y.T. Yeh, K. Gulino, Y.H. Zhang, A. Sabestien, T.W. Chou, B. Zhou, Z. Lin, I. Albert, H. Lu, V. Swaminathan, E. Ghedin, M. Terrones, A rapid and label-free platform for virus capture and identification from clinical samples, Proc. Natl. Acad. Sci. U. S. A. 117 (2020). https://doi.org/10.1073/pnas.1910113117.

[8] C. Hu, Y. Xiao, Y. Zou, L. Dai, Carbon-Based Metal-Free Electrocatalysis for Energy Conversion, Energy Storage, and Environmental Protection, Electrochem.

Energy Rev. 1 (2018) 84–112. https://doi.org/10.1007/s41918-018-0003-2.

[9] A.J. Appleby, Electrocatalysis of aqueous dioxygen reduction, J. Electroanal. Chem. 357 (1993) 117–179. https://doi.org/10.1016/0022-0728(93)80378-U.

[10] A. Baby, L. Trovato, C. Di Valentin, Single Atom Catalysts (SAC) trapped in defective and nitrogen-doped graphene supported on metal substrates, Carbon N. Y. 174 (2021) 772–788. https://doi.org/10.1016/j.carbon.2020.12.045.

[11] L. Zhang, Y. Jia, G. Gao, X. Yan, N. Chen, J. Chen, M.T. Soo, B. Wood, D. Yang, A. Du, X. Yao, Graphene Defects Trap Atomic Ni Species for Hydrogen and Oxygen Evolution Reactions, Chem. 4 (2018) 285–297. https://doi.org/10.1016/j.chempr.2017.12.005.

[12] C. Hu, L. Dai, Multifunctional Carbon-Based Metal-Free Electrocatalysts for Simultaneous Oxygen Reduction, Oxygen Evolution, and Hydrogen Evolution, Adv. Mater. 29 (2017) 1604942. https://doi.org/10.1002/adma.201604942.

[13] C. Hu, Q. Dai, L. Dai, Multifunctional carbon-based metal-free catalysts for advanced energy conversion and storage, Cell Reports Phys. Sci. 2 (2021) 100328. https://doi.org/10.1016/j.xcrp.2021.100328.

[14] R. Ma, G. Lin, Y. Zhou, Q. Liu, T. Zhang, G. Shan, M. Yang, J. Wang, A review of oxygen reduction mechanisms for metal-free carbon-based electrocatalysts, Npj Comput. Mater. 5 (2019) 78. https://doi.org/10.1038/s41524-019-0210-3.

[15] Y. Peng, A. Rendón-Patiño, A. Franconetti, J. Albero, A. Primo, H. García, Photocatalytic Overall Water Splitting Activity of Templateless Structured Graphitic Nanoparticles Obtained from Cyclodextrins, ACS Appl. Energy Mater. 3 (2020) 6623–6632. https://doi.org/10.1021/acsaem.0c00789.

[16] C. Hu, X. Chen, Q. Dai, M. Wang, L. Qu, L. Dai, Earth-abundant carbon catalysts for renewable generation of clean energy from sunlight and water, Nano Energy. 41 (2017) 367–376. https://doi.org/10.1016/j.nanoen.2017.09.029.

[17] H. Wang, J. Jia, P. Song, Q. Wang, D. Li, S. Min, C. Qian, L. Wang, Y.F. Li, C. Ma, T. Wu, J. Yuan, M. Antonietti, G.A. Ozin, Efficient Electrocatalytic Reduction of CO2 by Nitrogen-Doped Nanoporous Carbon/Carbon Nanotube

Membranes: A Step Towards the Electrochemical CO2 Refinery, Angew. Chemie - Int. Ed. 56 (2017) 7847–7852. https://doi.org/10.1002/anie.201703720.

[18] J. Liang, Z. Jiang, P.K. Wong, C.-S. Lee, Recent Progress on Carbon Nitride and Its Hybrid Photocatalysts for CO 2 Reduction, Sol. RRL. 5 (2021) 2000478. https://doi.org/10.1002/solr.202000478.

[19] Y. Liu, Y. Zhang, K. Cheng, X. Quan, X. Fan, Y. Su, S. Chen, H. Zhao, Y. Zhang, H. Yu, M.R. Hoffmann, Selective Electrochemical Reduction of Carbon Dioxide to Ethanol on a Boron- and Nitrogen-Co-doped Nanodiamond, Angew. Chemie - Int. Ed. 56 (2017) 15607–15611. https://doi.org/10.1002/anie.201706311.

[20] W. Li, M. Seredych, E. Rodríguez-Castellón, T.J. Bandosz, Metal-free Nanoporous Carbon as a Catalyst for Electrochemical Reduction of CO2 to CO and CH4, ChemSusChem. 9 (2016) 606–616. https://doi.org/10.1002/cssc.201501575.

[21] L.H. Zhang, F. Yu, N.R. Shiju, Carbon-Based Catalysts for Selective Electrochemical Nitrogen-to-Ammonia Conversion, ACS Sustain. Chem. Eng. 9 (2021) 7687–7703. https://doi.org/10.1021/acssuschemeng.1c00575.

[22] I. Harmanli, N. V. Tarakina, M. Antonietti, M. Oschatz, “Giant” Nitrogen Uptake in Ionic Liquids Confined in Carbon Pores, J. Am. Chem. Soc. 143 (2021) 9377–9384. https://doi.org/10.1021/jacs.1c00783.

[23] J. Quílez-Bermejo, E. Morallón, D. Cazorla-Amorós, Metal-free heteroatom-doped carbon-based catalysts for ORR. A critical assessment about the role of heteroatoms, Carbon N. Y. 165 (2020) 434–454. https://doi.org/10.1016/j.carbon.2020.04.068.

[24] D. Xue, H. Xia, W. Yan, J. Zhang, S. Mu, Defect Engineering on Carbon-Based Catalysts for Electrocatalytic CO2 Reduction, Nano-Micro Lett. 13 (2021). https://doi.org/10.1007/s40820-020-00538-7.

[25] J. Zhang, L. Dai, Nitrogen, Phosphorus, and Fluorine Tri-doped Graphene as a Multifunctional Catalyst for Self-Powered Electrochemical Water Splitting, Angew. Chemie - Int. Ed. 55 (2016) 13296–13300.

https://doi.org/10.1002/anie.201607405.

[26] U. Banin, N. Waiskopf, L. Hammarström, G. Boschloo, M. Freitag, E.M.J. Johansson, J. Sá, H. Tian, M.B. Johnston, L.M. Herz, R.L. Milot, M.G. Kanatzidis, W. Ke, I. Spanopoulos, K.L. Kohlstedt, G.C. Schatz, N. Lewis, T. Meyer, A.J. Nozik, M.C. Beard, F. Armstrong, C.F. Megarity, C.A. Schmuttenmaer, V.S. Batista, G.W. Brudvig, Nanotechnology for catalysis and solar energy conversion, Nanotechnology. 32 (2021) 042003. https://doi.org/10.1088/1361-6528/abbce8.

[27] W. Li, J. Liu, D. Zhao, Mesoporous materials for energy conversion and storage devices, Nat. Rev. Mater. 1 (2016) 16023. https://doi.org/10.1038/natrevmats.2016.23.

[28] G. Li, J. Sun, W. Hou, S. Jiang, Y. Huang, J. Geng, Three-dimensional porous carbon composites containing high sulfur nanoparticle content for high-performance lithium–sulfur batteries, Nat. Commun. 7 (2016) 10601. https://doi.org/10.1038/ncomms10601.

[29] W. Zhang, Y. Wu, H.W. Bahng, Y. Cao, C. Yi, Y. Saygili, J. Luo, Y. Liu, L. Kavan, J.E. Moser, A. Hagfeldt, H. Tian, S.M. Zakeeruddin, W.H. Zhu, M. Grätzel, Comprehensive control of voltage loss enables 11.7% efficient solid-state dye-sensitized solar cells, Energy Environ. Sci. 11 (2018) 1779–1787. https://doi.org/10.1039/c8ee00661j.

[30] H. Wang, X. Liu, P. Niu, S. Wang, J. Shi, L. Li, Porous Two-Dimensional Materials for Photocatalytic and Electrocatalytic Applications, Matter. 2 (2020) 1377–1413. https://doi.org/10.1016/j.matt.2020.04.002.

[31] A.S. Mestre, A. Nabiço, P.L. Figueiredo, M.L. Pinto, M.S.C.S. Santos, I.M. Fonseca, Enhanced clofibric acid removal by activated carbons: Water hardness as a key parameter, Chem. Eng. J. 286 (2016) 538–548. https://doi.org/10.1016/j.cej.2015.10.066.

[32] T.C. Alves, A. Cabrera-Codony, D. Barceló, S. Rodriguez-Mozaz, A. Pinheiro, R. Gonzalez-Olmos, Influencing factors on the removal of pharmaceuticals from water with micro-grain activated carbon, Water Res. 144 (2018) 402–412.

https://doi.org/10.1016/j.watres.2018.07.037.

[33] P.C. Rúa-Gómez, A.A. Guedez, C.O. Ania, W. Püttmann, Upgrading of wastewater treatment plants through the use of unconventional treatment technologies: Removal of lidocaine, tramadol, venlafaxine and their metabolites, Water (Switzerland). 4 (2012) 650–669. https://doi.org/10.3390/w4030650.

[34] L. Dai, Carbon-Based Metal-Free Catalysts, Wiley-VCH Verlag GmbH & Co. KGaA, Weinheim, Germany, 2018. https://doi.org/10.1002/9783527811458.

[35] D.R. Dreyer, H.P. Jia, C.W. Bielawski, Graphene oxide: A convenient carbocatalyst for facilitating oxidation and hydration reactions, Angew. Chemie - Int. Ed. 49 (2010) 6813–6816. https://doi.org/10.1002/anie.201002160.

[36] I. Pelech, O.S.G.P. Soares, M.F.R. Pereira, J.L. Figueiredo, Oxidative dehydrogenation of isobutane on carbon xerogel catalysts, Catal. Today. 249 (2015) 176–183. https://doi.org/10.1016/j.cattod.2014.10.007.

[37] T.J. Bandosz, C.O. Ania, Origin and Perspectives of the Photochemical Activity of Nanoporous Carbons, Adv. Sci. 5 (2018) 1800293. https://doi.org/10.1002/advs.201800293.

[38] A. Gomis-Berenguer, J. Iniesta, A. Moro, V. Maurino, J.C. Lima, C.O. Ania, Boosting visible light conversion in the confined pore space of nanoporous carbons, Carbon N. Y. 96 (2016) 98–104. https://doi.org/10.1016/j.carbon.2015.09.047.

[39] N. Serpone, G. Sauvé, R. Koch, H. Tahiri, P. Pichat, P. Piccinini, E. Pelizzetti, H. Hidaka, Standardization protocol of process efficiencies and activation parameters in heterogeneous photocatalysis: Relative photonic efficiencies ζr, J. Photochem. Photobiol. A Chem. 94 (1996) 191–203. https://doi.org/10.1016/1010-6030(95)04223-7.

[40] C.O. Ania, P.A. Armstrong, T.J. Bandosz, F. Beguin, A.P. Carvalho, A. Celzard, E. Frackowiak, M.A. Gilarranz, K. László, J. Matos, M.F.R. Pereira, Engaging nanoporous carbons in “beyond adsorption” applications: Characterization, challenges and performance, Carbon N. Y. 164 (2020) 69–84. https://doi.org/10.1016/j.carbon.2020.03.056.

[41] M. Ilkaeva, I. Krivtsov, J.R. García, E. Díaz, S. Ordóñez, E.I. García-López, G. Marcì, L. Palmisano, M.I. Maldonado, S. Malato, Selective photocatalytic oxidation of 5-hydroxymethyl-2-furfural in aqueous suspension of polymeric carbon nitride and its adduct with H2O2 in a solar pilot plant, Catal. Today. 315 (2018) 138–148. https://doi.org/10.1016/j.cattod.2018.03.013.

[42] O. Garcia-Rodriguez, A. Villot, H. Olvera-Vargas, C. Gerente, Y. Andres, O. Lefebvre, Impact of the saturation level on the electrochemical regeneration of activated carbon in a single sequential reactor, Carbon N. Y. 163 (2020) 265–275. https://doi.org/10.1016/j.carbon.2020.02.041.

[43] M.J. Lima, A.M.T. Silva, C.G. Silva, J.L. Faria, A microfluidic reactor application for the continuous-flow photocatalytic selective synthesis of aromatic aldehydes, Appl. Catal. A Gen. 608 (2020) 117844. https://doi.org/10.1016/j.apcata.2020.117844.

[44] I. Salmerón, I. Oller, K. V. Plakas, S. Malato, Carbon-based cathodes degradation during electro-Fenton treatment at pilot scale: Changes in H2O2 electrogeneration, Chemosphere. 275 (2021) 129962. https://doi.org/10.1016/j.chemosphere.2021.129962.

[45] A. Ghaffarkhah, E. Hosseini, M. Kamkar, A.A. Sehat, S. Dordanihaghighi, A. Allahbakhsh, C. Kuur, M. Arjmand, Synthesis, Applications, and Prospects of Graphene Quantum Dots: A Comprehensive Review, Small. 18 (2022) 2102683. https://doi.org/10.1002/smll.202102683.

[46] Z. Kang, S.T. Lee, Carbon dots: Advances in nanocarbon applications, Nanoscale. 11 (2019) 19214–19224. https://doi.org/10.1039/c9nr05647e.

[47] X. Xu, R. Ray, Y. Gu, H.J. Ploehn, L. Gearheart, K. Raker, W.A. Scrivens, Electrophoretic analysis and purification of fluorescent single-walled carbon nanotube fragments, J. Am. Chem. Soc. 126 (2004) 12736–12737. https://doi.org/10.1021/ja040082h.

[48] L.A. Ponomarenko, F. Schedin, M.I. Katsnelson, R. Yang, E.W. Hill, K.S. Novoselov, A.K. Geim, Chaotic Dirac Billiard in Graphene Quantum Dots, Science (80-.). 320 (2008) 356–358. https://doi.org/10.1126/science.1154663.

[49] A. Bianco, H.M. Cheng, T. Enoki, Y. Gogotsi, R.H. Hurt, N. Koratkar, T. Kyotani, M. Monthioux, C.R. Park, J.M.D. Tascon, J. Zhang, All in the graphene family - A recommended nomenclature for two-dimensional carbon materials, Carbon N. Y. 65 (2013) 1–6. https://doi.org/10.1016/j.carbon.2013.08.038.

[50] B. Bartolomei, A. Bogo, F. Amato, G. Ragazzon, M. Prato, Nuclear Magnetic Resonance Reveals Molecular Species in Carbon Nanodot Samples Disclosing Flaws, Angew. Chemie Int. Ed. n/a (2022) e202200038. https://doi.org/https://doi.org/10.1002/anie.202200038.

[51] H. Ding, X.X. Zhou, J.S. Wei, X.B. Li, B.T. Qin, X.B. Chen, H.M. Xiong, Carbon dots with red/near-infrared emissions and their intrinsic merits for biomedical applications, Carbon N. Y. 167 (2020) 322–344. https://doi.org/10.1016/j.carbon.2020.06.024.

[52] C. Zhao, X. Song, Y. Liu, Y. Fu, L. Ye, N. Wang, F. Wang, L. Li, M. Mohammadniaei, M. Zhang, Q. Zhang, J. Liu, Synthesis of graphene quantum dots and their applications in drug delivery, J. Nanobiotechnology. 18 (2020). https://doi.org/10.1186/s12951-020-00698-z.

[53] M.R. Younis, G. He, J. Lin, P. Huang, Recent Advances on Graphene Quantum Dots for Bioimaging Applications, Front. Chem. 8 (2020). https://doi.org/10.3389/fchem.2020.00424.

[54] D.K. Ji, G. Reina, S. Guo, M. Eredia, P. Samorì, C. Ménard-Moyon, A. Bianco, Controlled functionalization of carbon nanodots for targeted intracellular production of reactive oxygen species, Nanoscale Horizons. 5 (2020) 1240–1249. https://doi.org/10.1039/d0nh00300j.

[55] H. Terrones, M. Terrones, W.K. Hsu, Beyond C60: graphite structures for the future, Chem. Soc. Rev. 24 (1995) 341. https://doi.org/10.1039/cs9952400341.

[56] T. Lenosky, X. Gonze, M. Teter, V. Elser, Energetics of negatively curved graphitic carbon, Nature. 355 (1992) 333–335. https://doi.org/10.1038/355333a0.

[57] A.L. MACKAY, H. TERRONES, Diamond from graphite, Nature. 352 (1991) 762–762. https://doi.org/10.1038/352762a0.

[58] H. Terrones, M. Terrones, Curved nanostructured materials, New J. Phys. 5 (2003) 126–126. https://doi.org/10.1088/1367-2630/5/1/126.

[59] M. O'Keeffe, G.B. Adams, O.F. Sankey, Predicted new low energy forms of carbon, Phys. Rev. Lett. 68 (1992) 2325–2328. https://doi.org/10.1103/PhysRevLett.68.2325.

[60] Y. Ito, Y. Tanabe, H.-J. Qiu, K. Sugawara, S. Heguri, N.H. Tu, K.K. Huynh, T. Fujita, T. Takahashi, K. Tanigaki, M. Chen, High-Quality Three-Dimensional Nanoporous Graphene, Angew. Chemie Int. Ed. 53 (2014) 4822–4826. https://doi.org/10.1002/anie.201402662.

[61] Y. Wu, N. Yi, L. Huang, T. Zhang, S. Fang, H. Chang, N. Li, J. Oh, J.A. Lee, M. Kozlov, A.C. Chipara, H. Terrones, P. Xiao, G. Long, Y. Huang, F. Zhang, L. Zhang, X. Lepró, C. Haines, M.D. Lima, N.P. Lopez, L.P. Rajukumar, A.L. Elias, S. Feng, S.J. Kim, N.T. Narayanan, P.M. Ajayan, M. Terrones, A. Aliev, P. Chu, Z. Zhang, R.H. Baughman, Y. Chen, Three-dimensionally bonded spongy graphene material with super compressive elasticity and near-zero Poisson's ratio, Nat. Commun. 6 (2015) 6141. https://doi.org/10.1038/ncomms7141.

[62] Y. Zhu, L. Li, C. Zhang, G. Casillas, Z. Sun, Z. Yan, G. Ruan, Z. Peng, A.-R.O. Raji, C. Kittrell, R.H. Hauge, J.M. Tour, A seamless three-dimensional carbon nanotube graphene hybrid material, Nat. Commun. 3 (2012) 1225. https://doi.org/10.1038/ncomms2234.

[63] Z. Qin, G.S. Jung, M.J. Kang, M.J. Buehler, The mechanics and design of a lightweight three-dimensional graphene assembly, Sci. Adv. 3 (2017). https://doi.org/10.1126/sciadv.1601536.

[64] O. Al-Ketan, A. Soliman, A.M. AlQubaisi, R.K. Abu Al-Rub, Nature-Inspired Lightweight Cellular Co-Continuous Composites with Architected Periodic Gyroidal Structures, Adv. Eng. Mater. 20 (2018) 1700549. https://doi.org/10.1002/adem.201700549.

[65] S.M. Sajadi, P.S. Owuor, S. Schara, C.F. Woellner, V. Rodrigues, R. Vajtai, J. Lou, D.S. Galvão, C.S. Tiwary, P.M. Ajayan, Multiscale Geometric Design Principles Applied to 3D Printed Schwarzites, Adv. Mater. 30 (2018) 1704820.

https://doi.org/10.1002/adma.201704820.

[66] V. Meunier, A.G. Souza Filho, E.B. Barros, M.S. Dresselhaus, Physical properties of low-dimensional sp2 -based carbon nanostructures, Rev. Mod. Phys. 88 (2016) 025005. https://doi.org/10.1103/RevModPhys.88.025005.

[67] J.M. Romo-Herrera, M. Terrones, H. Terrones, S. Dag, V. Meunier, Covalent {2D} and {3D} networks from {1D} nanostructures: {Designing} new materials, Nano Lett. 7 (2007) 570–576. https://doi.org/10.1021/nl0622202.

[68] S. Jiang, P.X. Hou, C. Liu, H.M. Cheng, High-performance single-wall carbon nanotube transparent conductive films, J. Mater. Sci. Technol. 35 (2019) 2447–2462. https://doi.org/10.1016/j.jmst.2019.07.011.

[69] Z. Wu, Z. Chen, X. Du, J.M. Logan, J. Sippel, M. Nikolou, K. Kamaras, J.R. Reynolds, D.B. Tanner, A.F. Hebard, A.G. Rinzler, Transparent, conductive carbon nanotube films, Science (80-.). 305 (2004) 1273–1276. https://doi.org/10.1126/science.1101243.

[70] J.W. Jo, J.W. Jung, J.U. Lee, W.H. Jo, Fabrication of highly conductive and transparent thin films from single-walled carbon nanotubes using a new non-ionic surfactant via spin coating, ACS Nano. 4 (2010) 5382–5388. https://doi.org/10.1021/nn1009837.

[71] Y. Kim, N. Minami, W. Zhu, S. Kazaoui, R. Azumi, M. Matsumoto, Langmuir-Blodgett Films of Single-Wall Carbon Nanotubes: Layer-by-Layer Deposition and In-plane Orientation of Tubes, Japanese J. Appl. Physics, Part 1 Regul. Pap. Short Notes Rev. Pap. 42 (2003) 7629–7634. https://doi.org/10.1143/jjap.42.7629.

[72] N. Saran, K. Parikh, D.S. Suh, E. Muñoz, H. Kolla, S.K. Manohar, Fabrication and Characterization of Thin Films of Single-Walled Carbon Nanotube Bundles on Flexible Plastic Substrates, J. Am. Chem. Soc. 126 (2004) 4462–4463. https://doi.org/10.1021/ja037273p.

[73] R.C. Tenent, T.M. Barnes, J.D. Bergeson, A.J. Ferguson, B. To, L.M. Gedvilas, M.J. Heben, J.L. Blackburn, UItrasmooth, large-area, high-uniformity, conductive transparent single-walled-carbon-nanotube films for photovoltaics

produced by ultrasonic spraying, Adv. Mater. 21 (2009) 3210–3216. https://doi.org/10.1002/adma.200803551.

[74] B. Dan, G.C. Irvin, M. Pasquali, Continuous and scalable fabrication of transparent conducting carbon nanotube films, ACS Nano. 3 (2009) 835–843. https://doi.org/10.1021/nn8008307.

[75] A. Kaskela, A.G. Nasibulin, M.Y. Timmermans, B. Aitchison, A. Papadimitratos, Y. Tian, Z. Zhu, H. Jiang, D.P. Brown, A. Zakhidov, E.I. Kauppinen, Aerosol-synthesized SWCNT networks with tunable conductivity and transparency by a dry transfer technique, Nano Lett. 10 (2010) 4349–4355. https://doi.org/10.1021/nl101680s.

[76] S. Jiang, P.-X. Hou, M.-L. Chen, B.-W. Wang, D.-M. Sun, D.-M. Tang, Q. Jin, Q.-X. Guo, D.-D. Zhang, J.-H. Du, K.-P. Tai, J. Tan, E.I. Kauppinen, C. Liu, H.-M. Cheng, Ultrahigh-performance transparent conductive films of carbon-welded isolated single-wall carbon nanotubes., Sci. Adv. 4 (2018) eaap9264. https://doi.org/10.1126/sciadv.aap9264.

[77] T.M. Barnes, J.L. Blackburn, J. van de Lagemaat, T.J. Coutts, M.J. Heben, Reversibility, dopant desorption, and tunneling in the temperature-dependent conductivity of type-separated, conductive carbon nanotube networks, ACS Nano. 2 (2008) 1968–1976. https://doi.org/10.1021/nn800194u.

[78] B.C. Edwards, Design and deployment of a space elevator, Acta Astronaut. 47 (2000) 735–744. https://doi.org/10.1016/S0094-5765(00)00111-9.

[79] H.M. Cheng, F. Li, X. Sun, S.D.M. Brown, M.A. Pimenta, A. Marucci, G. Dresselhaus, M.S. Dresselhaus, Bulk morphology and diameter distribution of single-walled carbon nanotubes synthesized by catalytic decomposition of hydrocarbons, Chem. Phys. Lett. 289 (1998) 602–610. https://doi.org/10.1016/S0009-2614(98)00479-5.

[80] H.W. Zhu, C.L. Xu, D.H. Wu, B.Q. Wei, R. Vajtai, P.M. Ajayan, Direct synthesis of long single-walled carbon nanotube strands, Science (80-.). 296 (2002) 884–886. https://doi.org/10.1126/science.1066996.

[81] C. Liu, H.M. Cheng, H.T. Cong, F. Li, G. Su, H.L. Zhou, M.S. Dresselhaus,

Synthesis of macroscopically long ropes of well-aligned single-walled carbon nanotubes, Adv. Mater. 12 (2000) 1190–1192. https://doi.org/10.1002/1521-4095(200008)12:16<1190::AID-ADMA1190>3.0.CO;2-C.

[82] F. Li, H.M. Cheng, S. Bai, G. Su, M.S. Dresselhaus, Tensile strength of single-walled carbon nanotubes directly measured from their macroscopic ropes, Appl. Phys. Lett. 77 (2000) 3161–3163. https://doi.org/10.1063/1.1324984.

[83] L.M. Ericson, H. Fan, H. Peng, V.A. Davis, W. Zhou, J. Sulpizio, Y. Wang, R. Booker, J. Vavro, C. Guthy, A.N.G. Parra-Vasquez, M.J. Kim, S. Ramesh, R.K. Saini, C. Kittrell, G. Lavin, H. Schmidt, W.W. Adams, W.E. Billups, M. Pasquali, W.F. Hwang, R.H. Hauge, J.E. Fischer, R.E. Smalley, Macroscopic, neat, single-walled carbon nanotube fibers, Science (80-.). 305 (2004) 1447–1450. https://doi.org/10.1126/science.1101398.

[84] L.W. Taylor, O.S. Dewey, R.J. Headrick, N. Komatsu, N.M. Peraca, G. Wehmeyer, J. Kono, M. Pasquali, Improved properties, increased production, and the path to broad adoption of carbon nanotube fibers, Carbon N. Y. 171 (2021) 689–694. https://doi.org/10.1016/j.carbon.2020.07.058.

[85] N. Behabtu, C.C. Young, D.E. Tsentalovich, O. Kleinerman, X. Wang, A.W.K. Ma, E.A. Bengio, R.F. Ter Waarbeek, J.J. De Jong, R.E. Hoogerwerf, S.B. Fairchild, J.B. Ferguson, B. Maruyama, J. Kono, Y. Talmon, Y. Cohen, M.J. Otto, M. Pasquali, Strong, light, multifunctional fibers of carbon nanotubes with ultrahigh conductivity, Science (80-.). 339 (2013) 182–186. https://doi.org/10.1126/science.1228061.

[86] W. Lu, M. Zu, J.H. Byun, B.S. Kim, T.W. Chou, State of the art of carbon nanotube fibers: Opportunities and challenges, Adv. Mater. 24 (2012) 1805–1833. https://doi.org/10.1002/adma.201104672.

[87] D. Janas, A.P. Herman, S. Boncel, K.K.K. Koziol, Iodine monochloride as a powerful enhancer of electrical conductivity of carbon nanotube wires, Carbon N. Y. 73 (2014) 225–233. https://doi.org/10.1016/j.carbon.2014.02.058.

[88] H.W. Kroto, J.R. Heath, S.C. O'Brien, R.F. Curl, R.E. Smalley, C60: Buckminsterfullerene, Nature. 318 (1985) 162–163.

https://doi.org/10.1038/318162a0.

[89] S. Iijima, Helical microtubules of graphitic carbon, Nature. 354 (1991) 56–58. https://doi.org/10.1038/354056a0.

[90] M.F. El-Kady, V. Strong, S. Dubin, R.B. Kaner, Laser scribing of high-performance and flexible graphene-based electrochemical capacitors, Science (80-.). 335 (2012) 1326–1330. https://doi.org/10.1126/science.1216744.

[91] J. Lin, Z. Peng, Y. Liu, F. Ruiz-Zepeda, R. Ye, E.L.G. Samuel, M.J. Yacaman, B.I. Yakobson, J.M. Tour, Laser-induced porous graphene films from commercial polymers, Nat. Commun. 5 (2014) 5714. https://doi.org/10.1038/ncomms6714.

[92] R. Ye, D.K. James, J.M. Tour, Laser-Induced Graphene: From Discovery to Translation, Adv. Mater. 31 (2019) 1803621. https://doi.org/10.1002/adma.201803621.

[93] J.L. Beckham, J.T. Li, M.G. Stanford, W. Chen, E.A. McHugh, P.A. Advincula, K.M. Wyss, Y. Chyan, W.L. Boldman, P.D. Rack, J.M. Tour, High-Resolution Laser-Induced Graphene from Photoresist, ACS Nano. 15 (2021) 8976–8983. https://doi.org/10.1021/acsnano.1c01843.

[94] D.X. Luong, A.K. Subramanian, G.A.L. Silva, J. Yoon, S. Cofer, K. Yang, P.S. Owuor, T. Wang, Z. Wang, J. Lou, P.M. Ajayan, J.M. Tour, Laminated Object Manufacturing of 3D-Printed Laser-Induced Graphene Foams, Adv. Mater. 30 (2018) 1707416. https://doi.org/10.1002/adma.201707416.

[95] Y. Yao, K.K. Fu, S. Zhu, J. Dai, Y. Wang, G. Pastel, Y. Chen, T. Li, C. Wang, T. Li, L. Hu, Carbon Welding by Ultrafast Joule Heating, Nano Lett. 16 (2016) 7282–7289. https://doi.org/10.1021/acs.nanolett.6b03888.

[96] Y. Chen, K. Fu, S. Zhu, W. Luo, Y. Wang, Y. Li, E. Hitz, Y. Yao, J. Dai, J. Wan, V.A. Danner, T. Li, L. Hu, Reduced graphene oxide films with ultrahigh conductivity as Li-ion battery current collectors, Nano Lett. 16 (2016) 3616–3623. https://doi.org/10.1021/acs.nanolett.6b00743.

[97] X. Jia, M. Hofmann, V. Meunier, B.G. Sumpter, J. Campos-Delgado, J.M.

Romo-Herrera, H. Son, Y.-P. Hsieh, A. Reina, J. Kong, M. Terrones, M.S. Dresselhaus, Controlled formation of sharp zigzag and armchair edges in graphitic nanoribbons, Science (80-.). 323 (2009) 1701–1705. https://doi.org/10.1126/science.1166862.

[98] Y. Liu, P. Li, F. Wang, W. Fang, Z. Xu, W. Gao, C. Gao, Rapid roll-to-roll production of graphene film using intensive Joule heating, Carbon N. Y. 155 (2019) 462–468. https://doi.org/10.1016/j.carbon.2019.09.021.

[99] Y. Yao, Z. Huang, P. Xie, S.D. Lacey, R.J. Jacob, H. Xie, F. Chen, A. Nie, T. Pu, M. Rehwoldt, D. Yu, M.R. Zachariah, C. Wang, R. Shahbazian-Yassar, J. Li, L. Hu, Carbothermal shock synthesis of high-entropy-alloy nanoparticles, Science (80-.). 359 (2018) 1489–1494. https://doi.org/10.1126/science.aan5412.

[100] Y. Yao, Z. Huang, P. Xie, L. Wu, L. Ma, T. Li, Z. Pang, M. Jiao, Z. Liang, J. Gao, Y. He, D.J. Kline, M.R. Zachariah, C. Wang, J. Lu, T. Wu, T. Li, C. Wang, R. Shahbazian-Yassar, L. Hu, High temperature shockwave stabilized single atoms, Nat. Nanotechnol. 14 (2019) 851–857. https://doi.org/10.1038/s41565-019-0518-7.

[101] C. Wang, W. Ping, Q. Bai, H. Cui, R. Hensleigh, R. Wang, A.H. Brozena, Z. Xu, J. Dai, Y. Pei, C. Zheng, G. Pastel, J. Gao, X. Wang, H. Wang, J.C. Zhao, B. Yang, X. Zheng, J. Luo, Y. Mo, B. Dunn, L. Hu, A general method to synthesize and sinter bulk ceramics in seconds, Science (80-.). 368 (2020) 521–526. https://doi.org/10.1126/science.aaz7681.

[102] D.X. Luong, K. V. Bets, W.A. Algozeeb, M.G. Stanford, C. Kittrell, W. Chen, R. V. Salvatierra, M. Ren, E.A. McHugh, P.A. Advincula, Z. Wang, M. Bhatt, H. Guo, V. Mancevski, R. Shahsavari, B.I. Yakobson, J.M. Tour, Gram-scale bottom-up flash graphene synthesis, Nature. 577 (2020) 647–651. https://doi.org/10.1038/s41586-020-1938-0.

[103] K.M. Wyss, J.L. Beckham, W. Chen, D.X. Luong, P. Hundi, S. Raghuraman, R. Shahsavari, J.M. Tour, Converting plastic waste pyrolysis ash into flash graphene, Carbon N. Y. 174 (2021) 430–438. https://doi.org/10.1016/j.carbon.2020.12.063.

[104] P.A. Advincula, D.X. Luong, W. Chen, S. Raghuraman, R. Shahsavari, J.M. Tour, Flash graphene from rubber waste, Carbon N. Y. 178 (2021) 649–656. https://doi.org/10.1016/j.carbon.2021.03.020.

[105] B.I. Yakobson, J.M. Tour, M.G. Stanford, K. V. Bets, D.X. Luong, P.A. Advincula, W. Chen, J.T. Li, Z. Wang, E.A. McHugh, W.A. Algozeeb, Flash graphene morphologies, ACS Nano. 14 (2020) 13691–13699. https://doi.org/10.1021/acsnano.0c05900.

[106] W. Chen, J.T. Li, Z. Wang, W.A. Algozeeb, D.X. Luong, C. Kittrell, E.A. McHugh, P.A. Advincula, K.M. Wyss, J.L. Beckham, M.G. Stanford, B. Jiang, J.M. Tour, Ultrafast and Controllable Phase Evolution by Flash Joule Heating, ACS Nano. 15 (2021) 11158–11167. https://doi.org/10.1021/acsnano.1c03536.

[107] C. De Cauwer, J. Van Mierlo, T. Coosemans, Energy consumption prediction for electric vehicles based on real-world data, Energies. 8 (2015) 8573–8593. https://doi.org/10.3390/en8088573.

[108] W. Johannisson, D. Zenkert, G. Lindbergh, Model of a structural battery and its potential for system level mass savings, Multifunct. Mater. 2 (2019) 035002. https://doi.org/10.1088/2399-7532/ab3bdd.

[109] G. Fredi, S. Jeschke, A. Boulaoued, J. Wallenstein, M. Rashidi, F. Liu, R. Harnden, D. Zenkert, J. Hagberg, G. Lindbergh, P. Johansson, L. Stievano, L.E. Asp, Graphitic microstructure and performance of carbon fibre Li-ion structural battery electrodes, Multifunct. Mater. 1 (2018) 015003. https://doi.org/10.1088/2399-7532/aab707.

[110] V. Meunier, J. Kephart, C. Roland, J. Bernholc, Ab initio investigations of lithium diffusion in carbon nanotube systems, Phys. Rev. Lett. 88 (2002) 755061–755064. https://www.scopus.com/inward/record.uri?eid=2-s2.0-0037127817&partnerID=40&md5=d55eee045433eccb15e6cbe00c41cb10.

[111] T. Iijima, K. Suzuki, Y. Matsuda, Electrodic characteristics of various carbon materials for lithium rechargeable batteries, Synth. Met. 73 (1995) 9–20. https://doi.org/10.1016/0379-6779(95)03290-8.

[112] P. Liu, E. Sherman, A. Jacobsen, Design and fabrication of multifunctional

structural batteries, J. Power Sources. 189 (2009) 646–650. https://doi.org/10.1016/j.jpowsour.2008.09.082.

[113] L.E. Asp, M. Johansson, G. Lindbergh, J. Xu, D. Zenkert, Structural battery composites: a review, Funct. Compos. Struct. 1 (2019) 042001. https://doi.org/10.1088/2631-6331/ab5571.

[114] L.E. Asp, A. Bismarck, G. Lindbergh, S. Leijonmarck, T. Carlson, M.H. Kjell, Structural battery half cell, a structural battery and their manufacture, 14/634,997, 2015.

[115] I. Srivastava, R.J. Mehta, Z.-Z. Yu, L. Schadler, N. Koratkar, Raman study of interfacial load transfer in graphene nanocomposites, Appl. Phys. Lett. 98 (2011) 063102. https://doi.org/10.1063/1.3552685.

[116] E. Jacques, M.H. Kjell, D. Zenkert, G. Lindbergh, M. Behm, M. Willgert, Impact of electrochemical cycling on the tensile properties of carbon fibres for structural lithium-ion composite batteries, Compos. Sci. Technol. 72 (2012) 792–798. https://doi.org/10.1016/j.compscitech.2012.02.006.

[117] S. Duan, A.H.S. Iyer, D. Carlstedt, F. Rittweger, A. Sharits, C. Maddox, K.R. Riemschneider, D. Mollenhauer, M. Colliander, F. Liu, L.E. Asp, Effect of lithiation on the elastic moduli of carbon fibres, Carbon N. Y. 185 (2021) 234–241. https://doi.org/10.1016/j.carbon.2021.09.037.

[118] N. Ihrner, W. Johannisson, F. Sieland, D. Zenkert, M. Johansson, Structural lithium ion battery electrolytes: Via reaction induced phase-separation, J. Mater. Chem. A. 5 (2017) 25652–25659. https://doi.org/10.1039/c7ta04684g.

[119] L.E. Asp, K. Bouton, D. Carlstedt, S. Duan, R. Harnden, W. Johannisson, M. Johansen, M.K.G. Johansson, G. Lindbergh, F. Liu, K. Peuvot, L.M. Schneider, J. Xu, D. Zenkert, A Structural Battery and its Multifunctional Performance, Adv. Energy Sustain. Res. 2 (2021) 2000093. https://doi.org/10.1002/aesr.202000093.

[120] E. Fitzer, K.H. Köchling, H.P. Boehm, H. Marsh, Recommended terminology for the description of carbon as a solid, Pure Appl. Chem. 67 (1995) 473–506. https://doi.org/10.1351/pac199567030473.

[121] A.W. Hull, A new method of X-ray crystal analysis, Phys. Rev. 10 (1917) 661–696. https://doi.org/10.1103/PhysRev.10.661.

[122] J.D. Bernal, W.L. Bragg, The structure of graphite, Proc. R. Soc. London. Ser. A, Contain. Pap. a Math. Phys. Character. 106 (1924) 749–773. https://doi.org/10.1098/rspa.1924.0101.

[123] H. Ott, Die Kristallstruktur des Graphits, Ann. Phys. 390 (1928) 81–109. https://doi.org/10.1002/andp.19283900104.

[124] H. Lipson, A.R. Stokes, A New Structure of Carbon, Nature. 149[1] T. (1942) 328–328. https://doi.org/10.1038/149328a0.

[125] H.S. Lipson, A.R. Stokes, W.L. Bragg, The structure of graphite, Proc. R. Soc. London. Ser. A. Math. Phys. Sci. 181 (1942) 101–105. https://doi.org/10.1098/rspa.1942.0063.

[126] G.E. Bacon, A note on the rhombohedral modification of graphite, Acta Crystallogr. 3 (1950) 320–320. https://doi.org/10.1107/s0365110x50000872.

[127] H. -P Boehm, U. Hofmann, Die rhomboedrische Modifikation des Graphits, ZAAC - J. Inorg. Gen. Chem. 278 (1955) 58–77. https://doi.org/10.1002/zaac.19552780109.

[128] E. Matuyama, Rate of transformation of rhombohedral graphite at high temperatures, Nature. 178 (1956) 1459–1460. https://doi.org/10.1038/1781459a0.

[129] F. Laves, Y. Baskin, On the Formation of the Rhombohedral Graphite Modification, Zeitschrift Fur Krist. - New Cryst. Struct. 107 (1956) 337–356. https://doi.org/10.1524/zkri.1956.107.5-6.337.

[130] H. Gasparoux, Modification des propriétés magnétiques du graphite par création de sequences rhomboédriques, Carbon N. Y. 5 (1967) 441–451. https://doi.org/10.1016/0008-6223(67)90021-8.

[131] H.A. Wilhelm, B. Croset, G. Medjahdi, Proportion and dispersion of rhombohedral sequences in the hexagonal structure of graphite powders, Carbon N. Y. 45 (2007) 2356–2364. https://doi.org/10.1016/j.carbon.2007.07.010.

[132] J.W. McClure, Electron energy band structure and electronic properties of rhombohedral graphite, Carbon N. Y. 7 (1969) 425–432. https://doi.org/10.1016/0008-6223(69)90073-6.

[133] R.R. Haering, Band Structure of Rhombohedral Graphite, Can. J. Phys. 36 (1958) 352–362. https://doi.org/10.1139/p58-036.

[134] J.C. Charlier, X. Gonze, J.P. Michenaud, First-principles study of the stacking effect on the electronic properties of graphite(s), Carbon N. Y. 32 (1994) 289–299. https://doi.org/10.1016/0008-6223(94)90192-9.

[135] M. Dadsetani, J.T. Titantah, D. Lamoen, Ab initio calculation of the energy-loss near-edge structure of some carbon allotropes: Comparison with n-diamond, Diam. Relat. Mater. 19 (2010) 73–77. https://doi.org/10.1016/j.diamond.2009.11.004.

[136] B. Wen, J. Zhao, T. Li, C. Dong, n-diamond: an intermediate state between rhombohedral graphite and diamond?, New J. Phys. 8 (2006) 62–62. https://doi.org/10.1088/1367-2630/8/5/062.

[137] S. Ganguli, A.K. Roy, D.P. Anderson, Improved thermal conductivity for chemically functionalized exfoliated graphite/epoxy composites, Carbon N. Y. 46 (2008) 806–817. https://doi.org/10.1016/j.carbon.2008.02.008.

[138] Q. Lin, T. Li, Z. Liu, Y. Song, L. He, Z. Hu, Q. Guo, H. Ye, High-resolution TEM observations of isolated rhombohedral crystallites in graphite blocks, Carbon N. Y. 50 (2012) 2369–2371. https://doi.org/10.1016/j.carbon.2012.01.054.

[139] A.N. Roviglione, J.D. Hermida, Rhombohedral Graphite Phase in Nodules from Ductile Cast Iron, Procedia Mater. Sci. 8 (2015) 924–933. https://doi.org/10.1016/j.mspro.2015.04.153.

[140] A. Ortiz-Morales, J. Ortiz-López, B. Leal-Acevedo, R. Gómez-Aguilar, Thermoluminescence of single wall carbon nanotubes synthesized by hydrogen-arc-discharge method, Appl. Radiat. Isot. 145 (2019) 32–38. https://doi.org/10.1016/j.apradiso.2018.11.001.

[141] D. Pierucci, T. Brumme, J.-C. Girard, M. Calandra, M.G. Silly, F. Sirotti, A. Barbier, F. Mauri, A. Ouerghi, Atomic and electronic structure of trilayer graphene/SiC(0001): Evidence of Strong Dependence on Stacking Sequence and charge transfer, Sci. Rep. 6 (2016) 33487. https://doi.org/10.1038/srep33487.

[142] X. Zhang, W.P. Han, X.F. Qiao, Q.H. Tan, Y.F. Wang, J. Zhang, P.H. Tan, Raman characterization of AB-and ABC-stacked few-layer graphene by interlayer shear modes, Carbon N. Y. 99 (2016) 118–122. https://doi.org/10.1016/j.carbon.2015.11.062.

[143] L. Liang, J. Zhang, B.G. Sumpter, Q.-H. Tan, P.-H. Tan, V. Meunier, Low-Frequency Shear and Layer-Breathing Modes in Raman Scattering of Two-Dimensional Materials, ACS Nano. 11 (2017) 11777–11802. https://doi.org/10.1021/acsnano.7b06551.

[144] T. Latychevskaia, S.-K. Son, Y. Yang, D. Chancellor, M. Brown, S. Ozdemir, I. Madan, G. Berruto, F. Carbone, A. Mishchenko, K.S. Novoselov, Stacking transition in rhombohedral graphite, Front. Phys. 14 (2019) 13608. https://doi.org/10.1007/s11467-018-0867-y.

[145] Y. Yang, Y.C. Zou, C.R. Woods, Y. Shi, J. Yin, S. Xu, S. Ozdemir, T. Taniguchi, K. Watanabe, A.K. Geim, K.S. Novoselov, S.J. Haigh, A. Mishchenko, Stacking Order in Graphite Films Controlled by van der Waals Technology, Nano Lett. 19 (2019) 8526–8532. https://doi.org/10.1021/acs.nanolett.9b03014.

[146] K.S. Novoselov, A. Mishchenko, A. Carvalho, A.H. Castro Neto, 2D materials and van der Waals heterostructures, Science (80-.). 353 (2016) aac9439. https://doi.org/10.1126/science.aac9439.

[147] Y. Shi, S. Xu, Y. Yang, S. Slizovskiy, S. V. Morozov, S.K. Son, S. Ozdemir, C. Mullan, J. Barrier, J. Yin, A.I. Berdyugin, B.A. Piot, T. Taniguchi, K. Watanabe, V.I. Fal'ko, K.S. Novoselov, A.K. Geim, A. Mishchenko, Electronic phase separation in multilayer rhombohedral graphite, Nature. 584 (2020) 210–214. https://doi.org/10.1038/s41586-020-2568-2.

[148] C.H. Xu, G.E. Scuseria, Theoretical predictions for a two-dimensional rhombohedral phase of solid C60, Phys. Rev. Lett. 74 (1995) 274–277.

https://doi.org/10.1103/PhysRevLett.74.274.

[149] K. Kamarás, Y. Iwasa, L. Forró, Erratum: Infrared spectra of one- and two-dimensional fullerene polymer structures: RbC60 and rhombohedral C60, Phys. Rev. B. 57 (1998) 5543–5543. https://doi.org/10.1103/PhysRevB.57.5543.

[150] T. Ferroir, L. Dubrovinsky, A. El Goresy, A. Simionovici, T. Nakamura, P. Gillet, Carbon polymorphism in shocked meteorites: Evidence for new natural ultrahard phases, Earth Planet. Sci. Lett. 290 (2010) 150–154. https://doi.org/10.1016/j.epsl.2009.12.015.

[151] S.F. Matar, V.L. Solozhenko, Ultra-hard rhombohedral carbon by crystal chemistry and ab initio investigations, J. Solid State Chem. 302 (2021) 122354. https://doi.org/10.1016/j.jssc.2021.122354.

[152] S.F. Matar, V.L. Solozhenko, Crystal chemistry rationale and ab initio investigation of ultra-hard dense rhombohedral carbon and boron nitride, Diam. Relat. Mater. 120 (2021) 108607. https://doi.org/10.1016/j.diamond.2021.108607.

[153] N.R. Laine, F.J. Vastola, P.L. Walker, The importance of active surface area in the carbon-oxygen reaction, in: J. Phys. Chem., 1963: pp. 2030–2034. https://doi.org/10.1021/j100804a016.

[154] J.P. Olivier, M. Winter, Determination of the absolute and relative extents of basal plane surface area and “non-basal plane surface” area of graphites and their impact on anode performance in lithium ion batteries, in: J. Power Sources, 2001: pp. 151–155. https://doi.org/10.1016/S0378-7753(01)00527-4.

[155] T. Ishii, S. Kashihara, Y. Hoshikawa, J.I. Ozaki, N. Kannari, K. Takai, T. Enoki, T. Kyotani, A quantitative analysis of carbon edge sites and an estimation of graphene sheet size in high-temperature treated, non-porous carbons, Carbon N. Y. 80 (2014) 135–145. https://doi.org/10.1016/j.carbon.2014.08.048.

[156] T. Ishii, Y. Kaburagi, A. Yoshida, Y. Hishiyama, H. Oka, N. Setoyama, J. ichi Ozaki, T. Kyotani, Analyses of trace amounts of edge sites in natural graphite, synthetic graphite and high-temperature treated coke for the understanding of their carbon molecular structures, Carbon N. Y. 125 (2017) 146–155.

https://doi.org/10.1016/j.carbon.2017.09.049.

[157] T. Ishii, J. ichi Ozaki, Understanding the chemical structure of carbon edge sites by using deuterium-labeled temperature-programmed desorption technique, Carbon N. Y. 161 (2020) 343–349. https://doi.org/10.1016/j.carbon.2020.01.079.

[158] G.B. Choi, S. Hong, J.H. Wee, D.W. Kim, T.H. Seo, K. Nomura, H. Nishihara, Y.A. Kim, Quantifying Carbon Edge Sites on Depressing Hydrogen Evolution Reaction Activity, Nano Lett. 20 (2020) 5885–5892. https://doi.org/10.1021/acs.nanolett.0c01842.

[159] R. Tang, K. Taguchi, H. Nishihara, T. Ishii, E. Morallón, D. Cazorla-Amorós, T. Asada, N. Kobayashi, Y. Muramatsu, T. Kyotani, Insight into the origin of carbon corrosion in positive electrodes of supercapacitors, J. Mater. Chem. A. 7 (2019) 7480–7488. https://doi.org/10.1039/C8TA11005K.

[160] K. Nomura, H. Nishihara, N. Kobayashi, T. Asada, T. Kyotani, 4.4 V Supercapacitors Based on Super-Stable Mesoporous Carbon Sheet Made of Edge-Free Graphene Walls, Energy Environ. Sci. 12 (2019) 1542–1549. https://doi.org/10.1039/c8ee03184c.

[161] J.H. Wee, K. Nomura, H. Nishihara, D.W. Kim, S. Hong, G.B. Choi, S.Y. Yeo, J.H. Kim, H.Y. Jung, Y.A. Kim, Edgeless porous carbon coating for durable and powerful lead-carbon batteries, Carbon N. Y. 185 (2021) 419–427. https://doi.org/10.1016/j.carbon.2021.09.046.

[162] M.A.N. Dewapriya, R.K.N.D. Rajapakse, W.P.S. Dias, Characterizing fracture stress of defective graphene samples using shallow and deep artificial neural networks, Carbon N. Y. 163 (2020) 425–440. https://doi.org/10.1016/j.carbon.2020.03.038.

[163] M. Čanađija, Deep learning framework for carbon nanotubes: Mechanical properties and modeling strategies, Carbon N. Y. 184 (2021) 891–901. https://doi.org/10.1016/j.carbon.2021.08.091.

[164] B. Mortazavi, I.S. Novikov, A. V Shapeev, A machine-learning-based investigation on the mechanical/failure response and thermal conductivity of semiconducting BC2N monolayers, Carbon N. Y. 188 (2022) 431–441.

https://doi.org/https://doi.org/10.1016/j.carbon.2021.12.039.

[165] D. Hedman, T. Rothe, G. Johansson, F. Sandin, J.A. Larsson, Y. Miyamoto, Impact of training and validation data on the performance of neural network potentials: A case study on carbon using the CA-9 dataset, Carbon Trends. 3 (2021). https://doi.org/10.1016/j.cartre.2021.100027.

[166] B. Mortazavi, A. Rajabpour, X. Zhuang, T. Rabczuk, A. V. Shapeev, Exploring thermal expansion of carbon-based nanosheets by machine-learning interatomic potentials, Carbon N. Y. 186 (2022) 501–508. https://doi.org/10.1016/j.carbon.2021.10.059.

[167] C. Cui, T. Ouyang, C. Tang, C. He, J. Li, C. Zhang, J. Zhong, Bayesian optimization-based design of defect gamma-graphyne nanoribbons with high thermoelectric conversion efficiency, Carbon N. Y. 176 (2021) 52–60. https://doi.org/10.1016/j.carbon.2021.01.126.

[168] P. Rowe, V.L. Deringer, P. Gasparotto, G. Csányi, A. Michaelides, An accurate and transferable machine learning potential for carbon, J. Chem. Phys. 153 (2020) 034702. https://doi.org/10.1063/5.0005084.

[169] B. Karasulu, J.-M. Leyssale, P. Rowe, C. Weber, C. de Tomas, Accelerating the prediction of large carbon clusters via structure search: Evaluation of machine-learning and classical potentials, Carbon N. Y. 191 (2022) 255–266. https://doi.org/https://doi.org/10.1016/j.carbon.2022.01.031.

[170] S. Singh, Z. Bin Junaid, V. Vyas, T.S. Kalyanwat, S.S. Rana, Identification of vacancy defects in carbon nanotubes using vibration analysis and machine learning, Carbon Trends. 5 (2021). https://doi.org/10.1016/j.cartre.2021.100091.

[171] N. Sheremetyeva, M. Lamparski, C. Daniels, B. Van Troeye, V. Meunier, Machine-learning models for Raman spectra analysis of twisted bilayer graphene, Carbon N. Y. 169 (2020) 455–464. https://doi.org/10.1016/j.carbon.2020.06.077.

[172] X. Chen, A. Bouhon, L. Li, F.M. Peeters, B. Sanyal, PAI-graphene: A new topological semimetallic two-dimensional carbon allotrope with highly tunable anisotropic Dirac cones, Carbon N. Y. 170 (2020) 477–486. https://doi.org/10.1016/j.carbon.2020.08.012.

[173] P. Rowe, G. Csányi, D. Alfè, A. Michaelides, Development of a machine learning potential for graphene, Phys. Rev. B. 97 (2018) 054303. https://doi.org/10.1103/PhysRevB.97.054303.

[174] V.L. Deringer, G. Csányi, Machine learning based interatomic potential for amorphous carbon, Phys. Rev. B. 95 (2017) 094203. https://doi.org/10.1103/PhysRevB.95.094203.

[175] H. Lin, S. Ye, X. Zhu, Geometry Orbital of Deep Learning (GOODLE): A uniform carbon potential, Carbon N. Y. 186 (2022) 313–319. https://doi.org/10.1016/j.carbon.2021.10.043.

[176] G.D. Förster, A. Castan, A. Loiseau, J. Nelayah, D. Alloyeau, F. Fossard, C. Bichara, H. Amara, A deep learning approach for determining the chiral indices of carbon nanotubes from high-resolution transmission electron microscopy images, Carbon N. Y. 169 (2020) 465–474. https://doi.org/10.1016/j.carbon.2020.06.086.

[177] D. Kumbhar, A. Palliyarayil, D. Reghu, D. Shrungar, S. Umapathy, S. Sil, Rapid discrimination of porous bio-carbon derived from nitrogen rich biomass using Raman spectroscopy and artificial intelligence methods, Carbon N. Y. 178 (2021) 792–802. https://doi.org/10.1016/j.carbon.2021.03.064.

[178] A. Kaushal, R. Alexander, P.T. Rao, J. Prakash, K. Dasgupta, Artificial neural network, Pareto optimization, and Taguchi analysis for the synthesis of single-walled carbon nanotubes, Carbon Trends. 2 (2021). https://doi.org/10.1016/j.cartre.2020.100016.

[179] H. Wahab, V. Jain, A.S. Tyrrell, M.A. Seas, L. Kotthoff, P.A. Johnson, Machine-learning-assisted fabrication: Bayesian optimization of laser-induced graphene patterning using in-situ Raman analysis, Carbon N. Y. 167 (2020) 609–619. https://doi.org/10.1016/j.carbon.2020.05.087.

[180] N. Shirolkar, P. Patwardhan, A. Rahman, A. Spear, S. Kumar, Investigating the efficacy of machine learning tools in modeling the continuous stabilization and carbonization process and predicting carbon fiber properties, Carbon N. Y. 174 (2021) 605–616. https://doi.org/10.1016/j.carbon.2020.12.044.

[181] M.I. Maulana Kusdhany, S.M. Lyth, New insights into hydrogen uptake on porous carbon materials via explainable machine learning, Carbon N. Y. 179 (2021) 190–201. https://doi.org/10.1016/j.carbon.2021.04.036.

Figures:

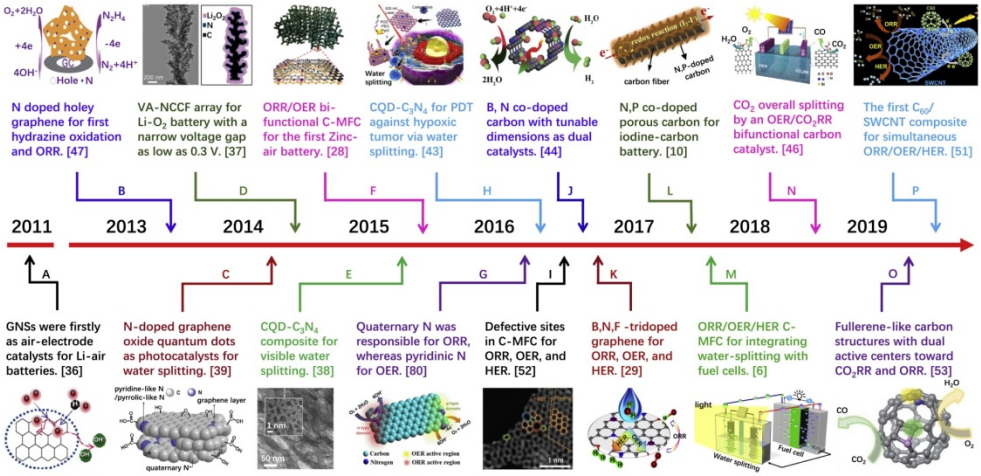

Figure 1: Timeline showing important developments in the application of metal-free carbons in electrocatalysis in the energy conversion field. Reprinted with permission from Ref. [13].

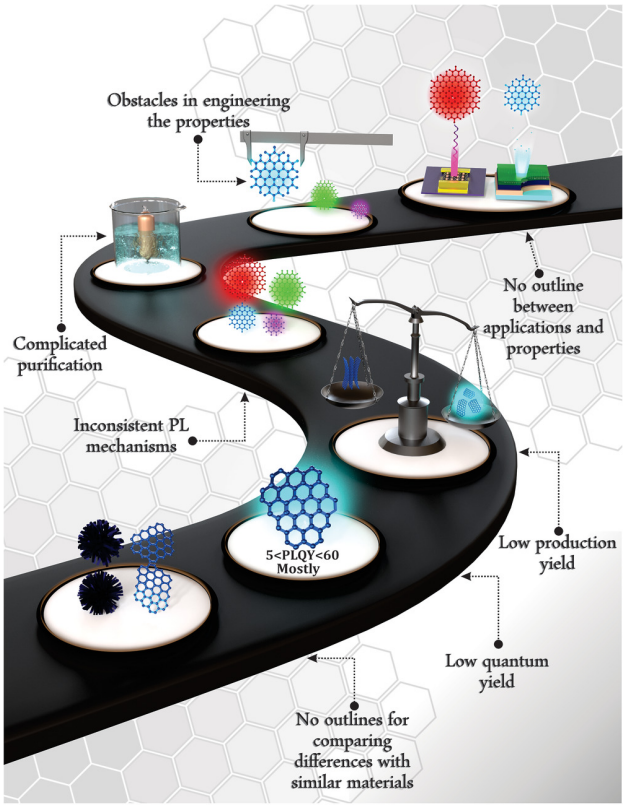

Figure 2: Current challenges and limitations of GQDs. Reproduced from Ref. [45] *with permission. Copyright 2021, Wiley-VCH.*

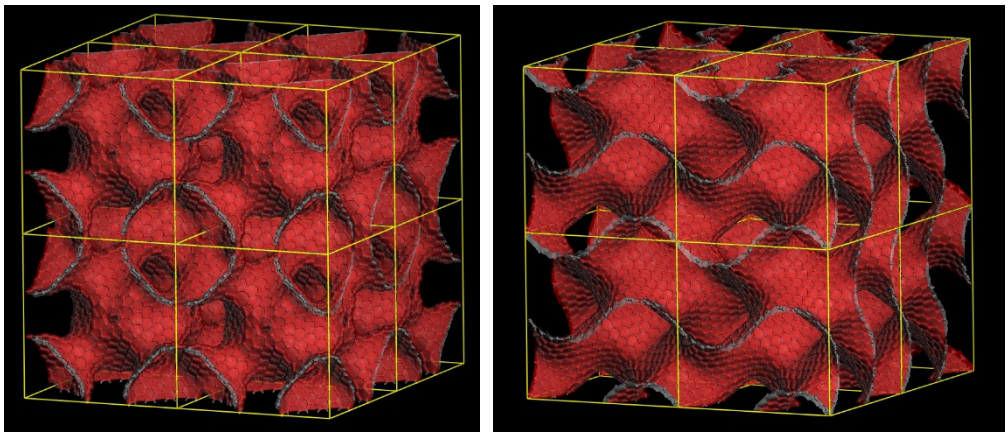

Figure 3: Molecular models of Schwarzites consisting of TPMS decorated with sp2 hybridized carbon atoms (courtesy of H. Terrones).

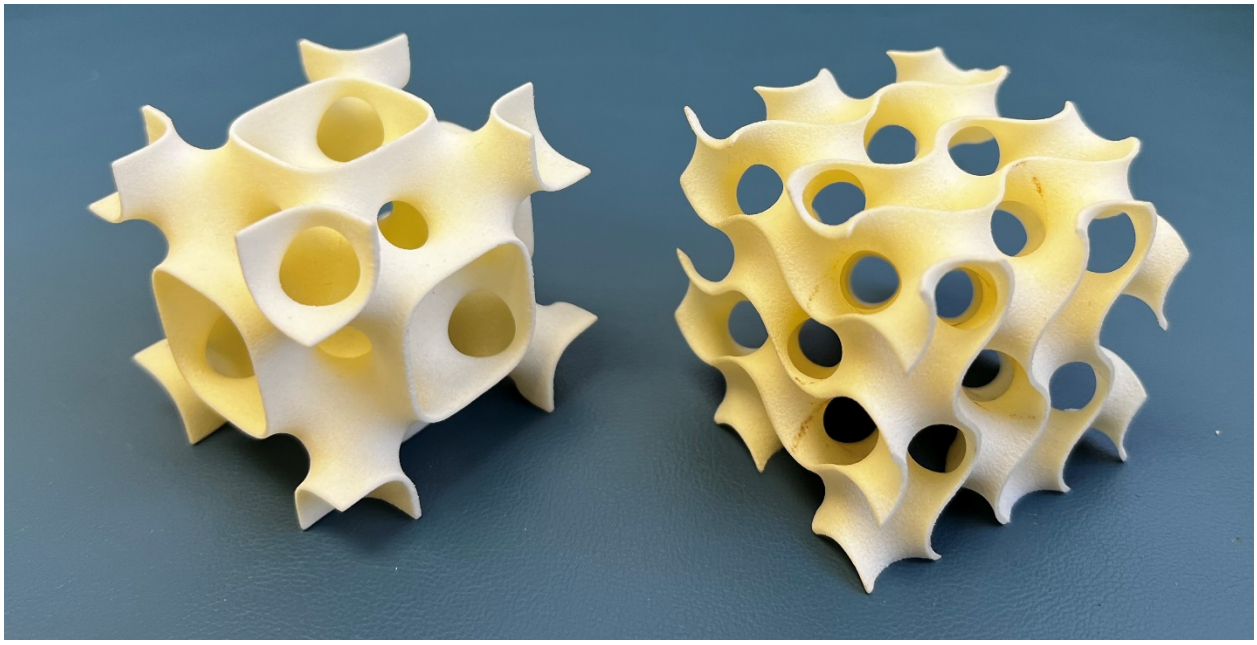

Figure 4: 3D polymer printed models of gyroid structures similar to those used by Buehler's group (models courtesy of A.L. Mackay).

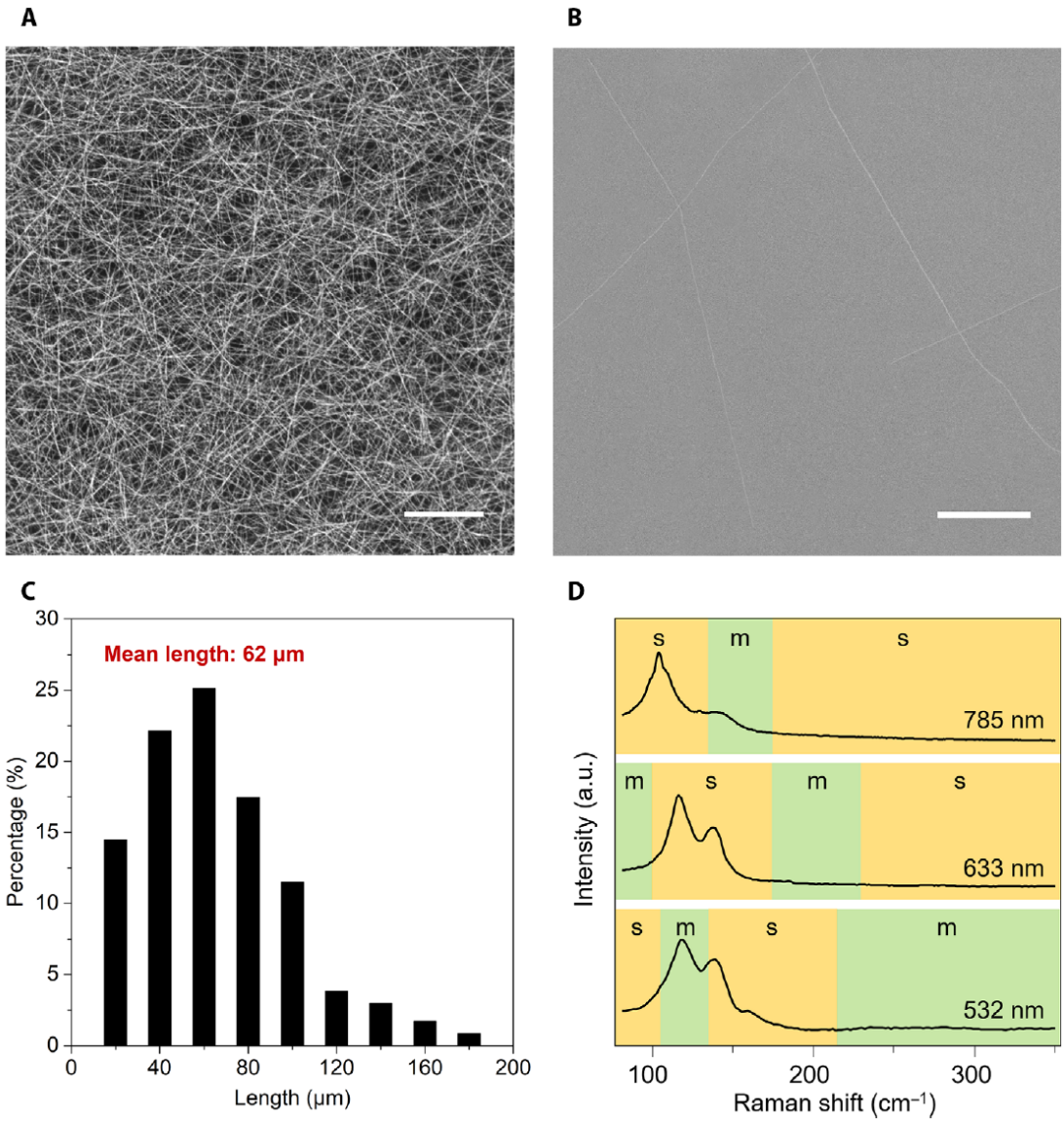

Figure 5: SEM images, length distribution, and Raman spectra of a SWCNT thin film composed of isolated and small-bundle nanotubes. (A-B) SEM images of SWCNT networks. Scale bars, 0.5 µm (A) and 10 µm (B). (C) Length distribution of the SWCNTs measured by SEM. (D) RBM mode Raman spectra of the SWCNTs excited by 532-, 633-, and 785-nm lasers.[76]

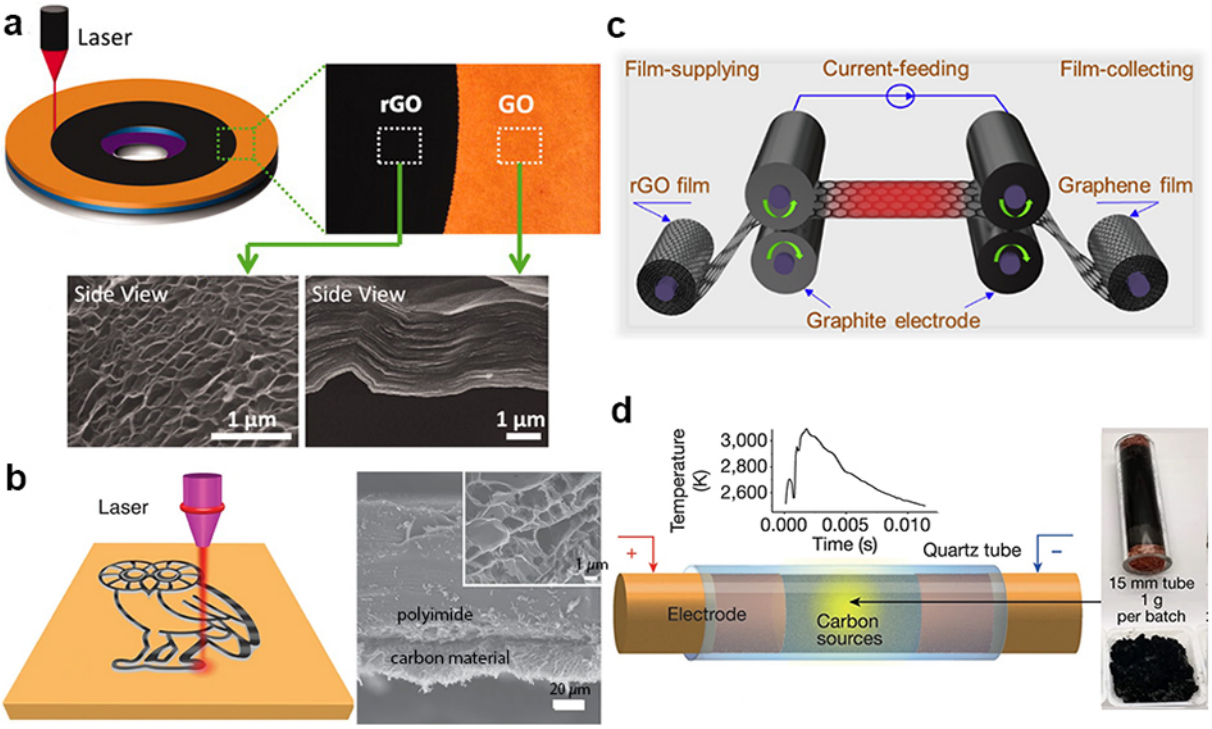

Figure 6: (a) Schematic illustration of GO film reduction by laser irradiation and SEM images of rGO and GO thin films. Adapted with permission from Ref.[90] *Copyright 2012, American Association for the Advancement of Science. (b) Schematic illustration of laser irritation on a polyimide film and Cross-sectional SEM of carbon materials synthesized on the polyimide film, the insert shows the porous structure of carbon materials. Adapted with permission from Ref.* [91]. *Copyright 2014, Springer Nature. (c) Schematic illustration of the roll-to-roll process to fabricate flexible rGO films. Adapted with permission from Ref.* [98]. *Copyright 2019, Elsevier B.V. (d) Schematic illustration of a new Joule heating process, the temperature rise vs. time plot, and a photo of the quartz tube reactor used and the resulting carbon material. Adapted with permission from Ref.* [102]. *Copyright 2020, Springer Nature.*

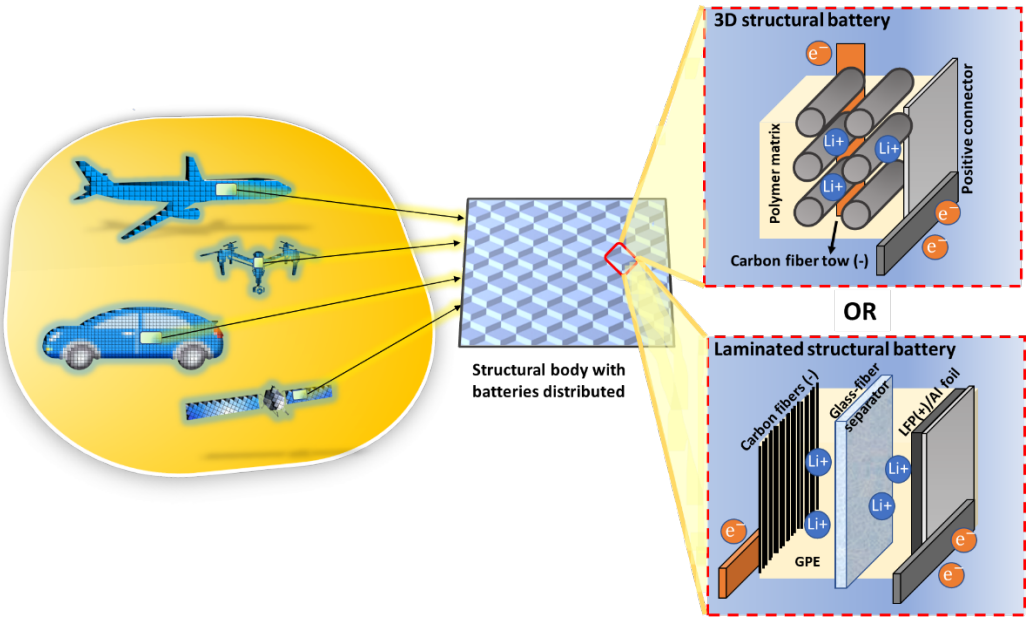

Figure 7: Illustration of structural battery concept: Laminated (below) and 3D fiber based (above) structural battery composite, using carbon fiber as anode and $LiFePO_4$ particles as cathode, along with polymer electrolyte matrix, for their application in automobiles and aerospace vehicles. [112–114]

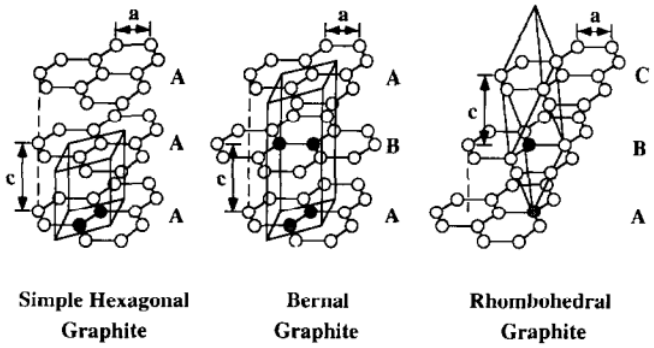

Figure 8: Comparison between three different graphitic structures: simple hexagonal (left), hexagonal (Bernal) (center), and rhombohedral (right) graphite. The unit cells are also shown in the different structures with their respective number of incorporated carbon atoms (grey). C is the interlayer distance, and a is the distance between nearest-neighbors. Adapted from ref. [134]*, with permission from Elsevier.*

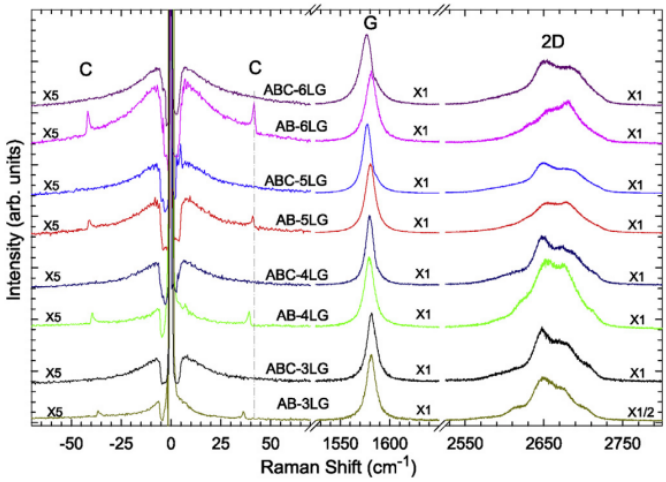

Figure 9: Raman spectra of ABA- and ABC-NLG (N = 3, 4, 5, 6) in the C, G and 2D peak spectral regions. The C modes are observed in ABA-NLG (N = 3, 4, 5, 6), but not in ABC-NLG. Adapted from ref. [142]*, with permission from Elsevier.*

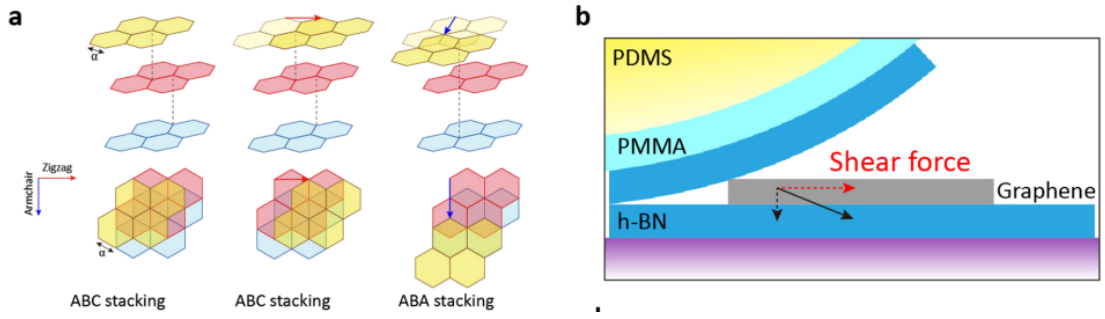

Figure 10: Stacking order control in graphite films. (a) Crystal structure and top view of the stacking order transformation of a model trilayer graphene. The top, middle, and bottom layers are labeled yellow, red, and blue, respectively. The left figure is the original ABC stacking trilayer. The middle and right figures are the final stacking order after the energetically favorable displacement of the top layer along zigzag (red arrow) and armchair (blue arrow) directions, respectively. α is the C−C bond length. (b) Schematic of the shear force applied to the flakes during micromechanical transfer. Adapted from ref. [145]*, with permission from ACS.*

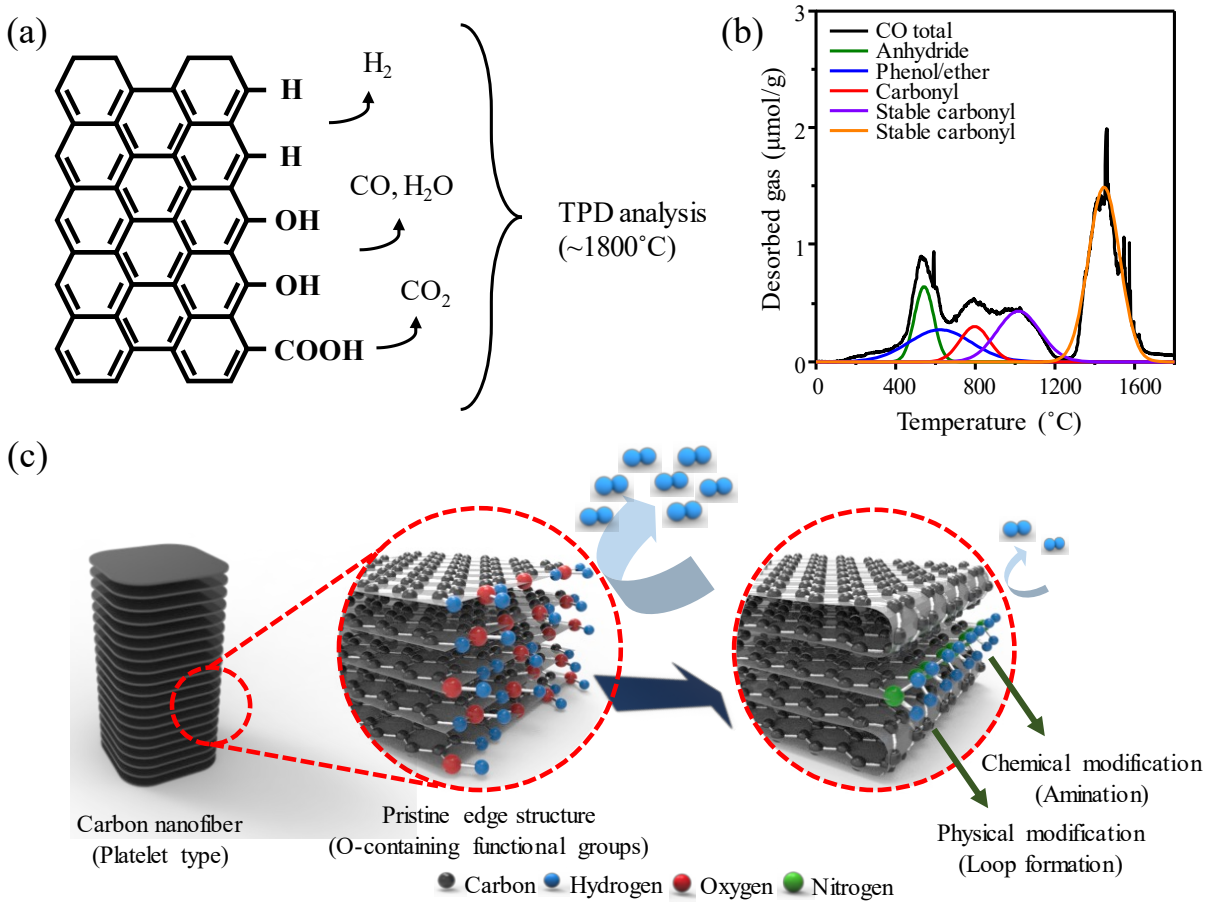

Figure 11: (a) Oxygen containing functional groups on the surface of carbon materials, (b) Peak fitting data of the deconvolution of CO desorption profiles using a multiple Gaussian function for the carbon nanofiber and (c) schematic illustration of depressing hydrogen evolution reaction via the physical and chemical passivation of edges. Adapted from ref. [158] *,with permission from ACS.*

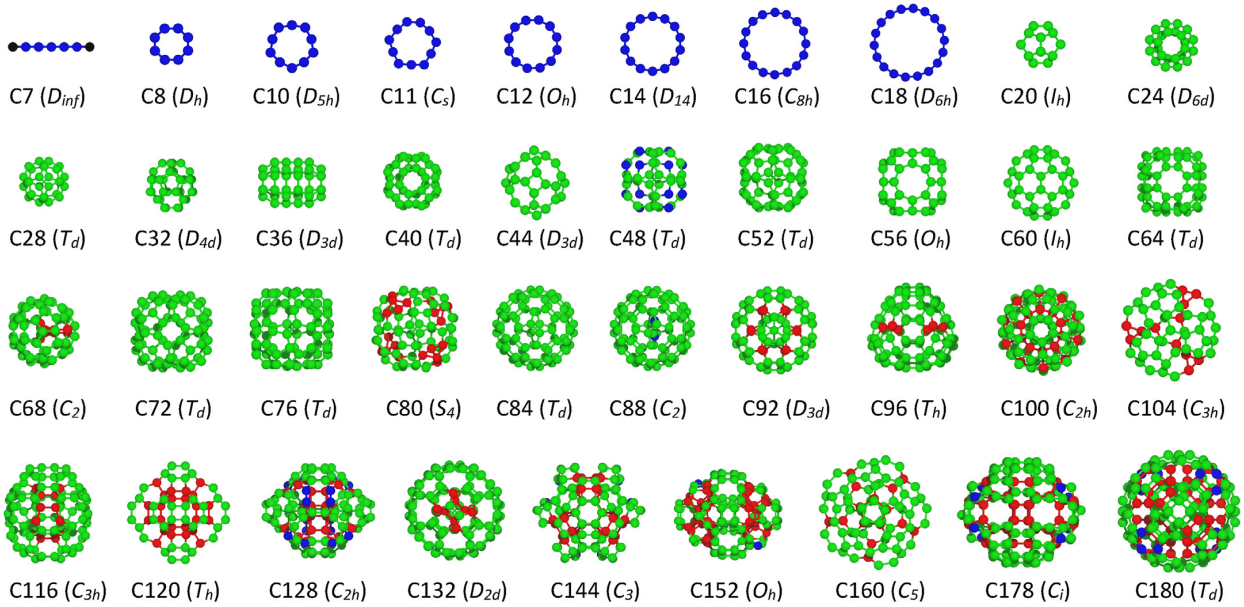

Figure 12: Visualization of the minimum-energy structures in a selection of ordered carbon clusters generated with AIRSS þ DFT. Clusters are labelled as Cn where n indicates the number of atoms. Point group symmetries are shown in parentheses. Carbon atoms are colored according to their hybridization: blue, green and red correspond to sp, sp2 and sp3, respectively. Reproduced from [169]